

Droplet Nucleation and Growth of Nanoparticles in the Flue Gas Cleaning Process

G. Cozzolino^{*/}, P. Sabia^{*}, M.de Joannon^{*}, R. Ragucci^{*}, A. Cavaliere^{**}**

^{*}Istituto di Ricerche sulla Combustione - C.N.R., Naples – ITALY

^{**}DICMAPI - Università Federico II, Naples – ITALY

Abstract

Control of particulate matter (PM) emissions from combustion facilities and industrial processes is important for protection of human health and environments. The aim of this work is to analyze the particles growth process, activated via heterogeneous water condensation mechanism, as a function of working conditions (temperature and vapor concentration), with particular emphasis on the effect of their dimension, number concentration, morphology and wettability on growth activation process.

The results demonstrate that higher inlet vapor concentration as well as lower working temperature increases the final size of the particles and reduce the induction time of process. In addition the presence in the system of higher wettable particles anticipates the occurrence of the characteristics time and improve the water uptake from gas flow. Furthermore the results were compared with some theoretical predictions with the purpose of verifying the effectiveness of the available models for the process characterization. In conclusion the characteristics times of droplet formation and growth process, experimentally evaluated, are compatible with practical applications and useful for the design of a real abatement unit.

Introduction

The efficiency of traditional physical separation processes, in removing particle with diameters ranging from 0.1 μm to 1 μm decrease to approximately 25%, thereby rendering their application impractical [1]. Improvements in the operation at optimal working conditions might be facilitated by increasing the dimension of the particles to be eliminated upstream of the standard cleaning processes. An innovative technique for both industrial applications relies on increasing the diameter of fine and ultra-fine particles by condensing water vapor onto the particles themselves. The easy availability of vapor at relatively low temperatures makes this technique interesting for a wide range of industries, including chemical, glass, cement and metallurgy production systems and combustion facilities, all of which are interested in the removal of fine particles from waste gases [2]. In the field of combustion process, this technique might be even more relevant for flue gases coming from MILD (Moderate or Intense Low-oxygen Dilution) [3] or coal Oxy-Fuel Combustion processes [4], where water vapor could be used as a diluent to reduce the maximum temperature reached during combustion, thereby leading to a decrease in pollutant formation. This study experimentally evaluated the evolution of droplets growth process as well as its characteristic time in dependence of working condition and particles properties.

Experimental configuration

The experimental set-up consists in a square cross section laminar flow chamber. A carrier gas, steam and/or particles from a spark generator system (PALAS GFG1000) are axially fed to the chamber with a 2 cm injection tube. An inert gas flow, is fed externally to the mainstream to prevent the diffusion of the droplets and particles toward the chamber walls and at the same time for a controlled cooling of the mainstream. A remotely controlled heater system avoids the steam condensation along the feed line. A thermocouple placed in proximity of the outflow section of the mainstream allows to control and monitoring the temperature of the working fluid. The results will be presented as a function of the axial coordinate i.e. residence time, t , being the axial flow velocity v constant and equal to 0.4 m/s in all the conditions reported. Accordingly, a residence time t_{res} equal for all the test cases to z_{max}/v , can be defined.

Profiles of polarization ratio have been obtained varying working condition (inlet temperature T_{in} vapor concentration $X_{v,\text{in}}$). Thus, $X_{v,\text{in}}=0$ corresponds to the case where only particles and carrier are fed to the flow chamber. By increasing the vapor concentration from 0 to 0.7, the percentage of the carrier gas has been changed in such way that the fluid-dynamic conditions are equivalent in all the condition considered. The confinement temperature was fixed at T_c of 298K. The aerosol generator is able produces graphite, iron and nickel particles with a monodispersed particle distribution with the maximum at $D_p=150$ nm, this diameter corresponds to a particle number density of $2 \cdot 10^7$ particle/cm³. The temporal evolution of the droplet growth process has been followed along the chamber axis (Z) by collecting the polarized components of laser light elastically scattered at 90° by the control volume and by computing the polarization ratio in dependence of operative conditions and particles characteristics. The final droplet dimension was assessed by comparing experimental data with numerical evaluation of polarization ratio computed through a Mie scattering coefficient program using Bruggeman approximation model [5]. Figure 1 shows the polarization ratio for composite droplet hosting a carbonaceous particle as a function of droplet size i.e. layer thickness, varying particle dispersion parametric in particles dispersion.

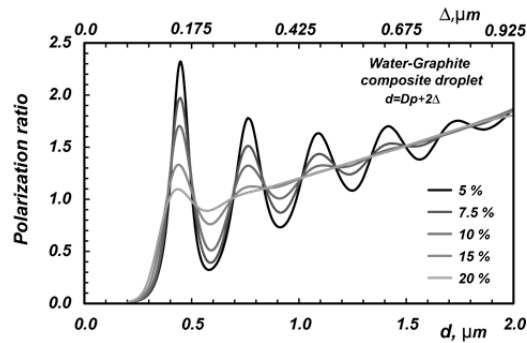


Figure 1. Polarization ratio of a composite droplet hosting a carbonaceous nanoparticle as a function of layer thickness parametric in particle dispersion

Theory

The fluid dynamic conditions typical of coaxial jet in laminar flow condition configuration, allows to evaluate the mixing degree between the core flow and confinement flow.

Once the local value of temperature T is measured, assuming a constant confinement flow temperature, it is possible to approximate the mixing degree as $\phi(T) = (T - T_c)/(T_{in} - T_c)$. In such a way the vapor local concentration may be reported as a function of the axial coordinate as $X_v = \phi(T) \cdot X_{v_{in}}$. The equilibrium vapor concentration of vapor bulk phase $X_{v_{sat}}$ was evaluated from $P_{sat} = P^\circ(T)$ (according to Antoine equation). This value is very close to equilibrium vapor concentration over particles surface evaluated from classical nucleation theory so it was not reported. Due to the complex morphology of particles their surface is very far from to be smooth, spherical and homogeneous as expected from Fletcher approximation [8]. On such a type of nano-structured surface the formation of negative curvature liquid meniscus, in the primary interparticle cavities, can be stabilized at subsaturation conditions with the respect of vapor bulk phase. In this case the equilibrium vapor concentration could be expressed as $P_H = P^\circ(T) \exp\left(\frac{M_w \sigma_{lv} H}{\rho_l R T}\right)$ where P_H is the equilibrium vapor pressure on a surface with negative curvature $H = 1/2r_k < 0$ where r_k is the Kelvin radius [6]. It is worth to note that the value of $X_{v_{sat}}(H)$ evaluated from the P_H strongly depends on surface morphology, chemical and physical properties of both particles and condensing vapor specie. The effect of more wettable particles i.e. smaller contact angle, leads to a decrease of P_H value.

Results and discussion

Figure 2(a) shows the polarization ratio and local values of vapor concentration evaluated with different theories above reported. In such a case a supersaturation condition is reported. The polarization ratio profile related to this working condition ($X_{v_{in}}=0.7$, $T_{in}=375K$ radial coordinate $r=10$ mm) shows a value very higher (>1) with the respect $X_{v_{in}}=0$ case [7], furthermore it shows an oscillating behavior along axial coordinate. In addition assuming a mono-disperse narrowed particle size distribution the oscillating behavior suggests that particles reach micronic size as supported by numeric model. The polarization ratio oscillations depend on the width of the size distribution function. As shown in Figure 1 the observation of three or more oscillations in correspondence of the drop size growth, due to water deposition on particle surface, is a clear indicator of a relatively narrow size dispersion of the droplets. As a consequence, it is possible to affirm that the activation of nucleation and growth occur contemporaneously on all particles (unitary activation efficiency).

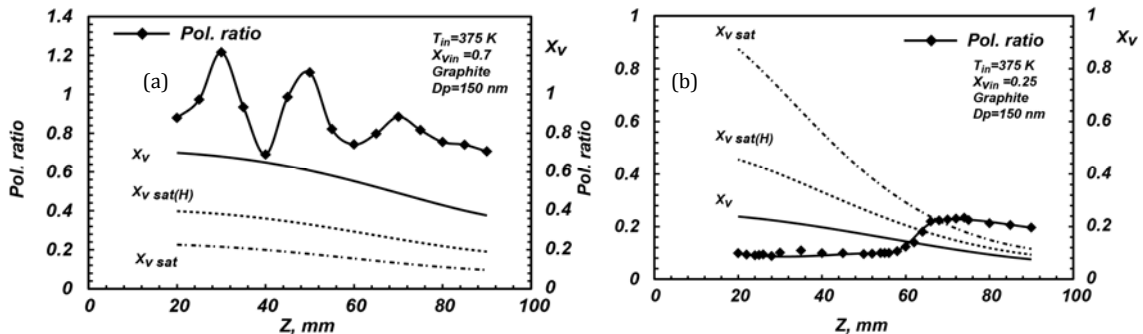


Figure 2. Left axis: Polarization ratio, right axis: X_v evaluated with different theory as a function of local temperature

In Figure 2(b) the profiles of polarization ratio and the local values of X_v , $X_{v_{sat}}$ and $X_{v_{sat}}(H)$ are reported. The trends of such vapor concentration profiles have been compared with the polarization ratio profile (secondary axis) measured for inlet condition of temperature and vapor concentration of $T_{in}=375$ K and $X_{v_{in}}=0.25$, feeding graphite particles into system and for a radial coordinate $r=0$ mm. It is clearly shown in the figure that the X_v is very low with respect to the saturation concentration needed for nucleation process as derived from classical nucleation theory in the

whole range considered. In Figure 2(b) the comparison of X_v and $X_{v_sat}(H)$ shows that they are relatively close especially in the spatial region where a change in polarization ratio occurs. When X_v approaches to $X_{v_sat}(H)$ the liquid begins to cover the particle so that an increase of scatterers' dimension is observed. This phenomenon allows to identify the induction time (t_{ind}) of the process, in correspondence of polarization ratio value variation. It begins to increase in correspondence of such conditions reaching a value of about 0.2 for $Z > 60$ mm. The droplet growth continues until the system reaches an equilibrium condition due to vapor depletion in the bulk phase, as showed from polarization ratio value that present a plateau up to $Z = 90$ mm. The polarization ratio profile reported in Figure 2(b) is typical of a small size variation in scatteres dimension due to low local relative humidity conditions. Sorjamaa et al., [9] by means of a theoretical analysis suggested that the process occurs due to adsorption of condensing species on particles even though no clear experimental identification of this process was available. Figure 3 shows the polarization ratio trends evaluated at $T_{in} = 405$ K for three value of inlet vapor concentration $X_{v,in} = 0, 0.25, 0.35$ and fed into the chamber graphite particle ($\theta = 85^\circ$), iron particles ($\theta = 50^\circ$) and nickel particles ($\theta = 20^\circ$). These data are the reported as function of residence time in order to underline the effect of particles wettability on characteristics time of droplet growth process. The results highlight that passing from graphite to nickel particles, (i.e. increasing particles wettability) the characteristics time of the process, for the same working conditions, decreases as suggested from polarization ratio profiles related to the different particles specie. For $X_v = 0.35$ the induction time varies from $t_{ind} = 0.15$ s for graphite, to 0.125 s, for iron and to 0.11s for nickel particles respectively. Furthermore higher particles wettability leads to higher coverage degree of particles by water layer. Again passing from graphite to nickel particles, polarization ratio reaches a maximum value of 0.4 for graphite, 0.58 for iron and 0.62 for nickel particles respectively. Same consideration apply for $X_v = 0.25$ condition. The final size of droplets was assessed in dependence of the operating condition and particles properties by means the effective refractive index model. At same time, by analyzing the temporal profile of polarization ratio, the induction time of droplet growth process was identified.

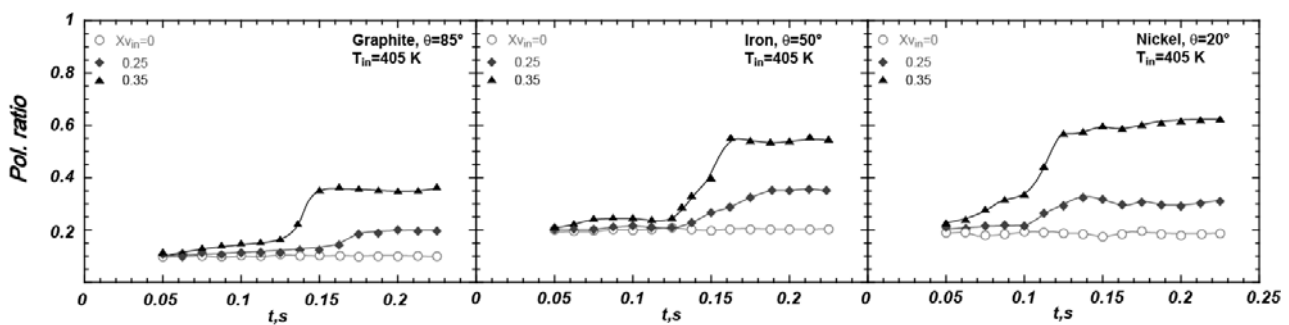


Figure 3: Polarization ratio trends for $T_{in} = 405$ K, $X_v = 0, 0.1, 0.25, 0.35$, varying the chemical specie of particle (i.e. contact angle) feeding to the system.

Conclusions

An evaluation of droplets growth process demonstrates that dispersed particles, acting as condensation nuclei, were captured in the nucleated water droplets with high efficiency. The main result obtained is that particle covering process related to its morphology and chemical properties is active at subsaturation condition, even if in this case the particle size variation is relatively low. On the other hand at supersaturation condition the nucleated droplet reaches a size of the order of micron. It is worthwhile to note that both mechanisms are particularly effective for particles capture showing an unitary activation efficiency in the operative conditions considered. The final size of the particles was increased with high inlet vapor concentrations and low working temperature. By increasing inlet vapor concentration from 0 up to 0.7, the final particle size increases, reaching a dimension greater than 1 micron; instead the induction time of droplet growth process decreases. Furthermore the presence in the system of more wettable particles results in lower induction time and higher water coverage. As final consideration, it is that the characteristic induction and growth times experimentally evaluated, are compatible with practical applications. Furthermore, their identification and the estimation can be very useful in the design and dimensioning of a real abatement units.

References

- [1] <http://www.epa.gov/apti/bces/module3/collect/collect.htm>
- [2] C. Ehrlich, G. Noll, W.-D. Kalkoff, G. Baumbach, A. Dreiseidler, Atmos. Environ., 41, 29, (2007), 6236-6254
- [3] A. Cavaliere, M. de Joannon, Prog. Energy Combust., 30 (2004), 329-366
- [4] B.J.P. Buhre, L.K. Elliott, C.D. Sheng, R.P. Gupta, T.F. Wall, Progr. Energ. Combust. Sci. 31 (2005) 283-307
- [5] G. Videen, D. Ngo, P. Chýlek, R. G. Pinnick, J. Opt. Soc. Am. A 12 (1995) 922-928.
- [6] F.M. Orr, L.E. Scriven, A.P. Rivas, J. Fluid Mech. 67 (1975) 723-742.
- [7] M. de Joannon, G. Cozzolino, A. Cavaliere, R. Ragucci, Fuel Process. Technol. 107, (2013) 113-118
- [8] Giechaskiel, X. Wang, D. Gilliland, Y. Drossinos, J. Aerosol. Sci. 42 (2011) 20-37.
- [9] R. Sorjamaa and A. Laaksonen, Atmos. Chem. Phys. 7 (2007) 6175-6180.

Droplet Nucleation and Growth of Nanoparticles in the Flue Gas Cleaning Process



Gennaro Cozzolino^{/**}*

P. Sabia^{}, M. de Joannon^{*}, R. Ragucci^{*}, A. Cavaliere^{**}*

**Istituto di Ricerche sulla Combustione - CNR, Naples, Italy*

*** DICMAPI - University Federico II, Naples, Italy*

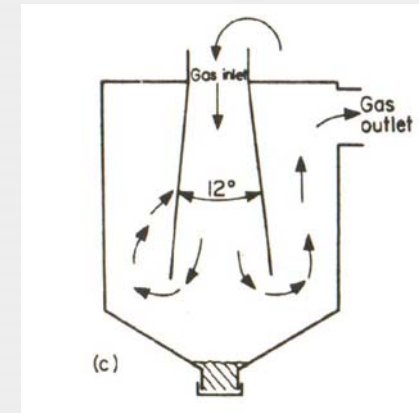
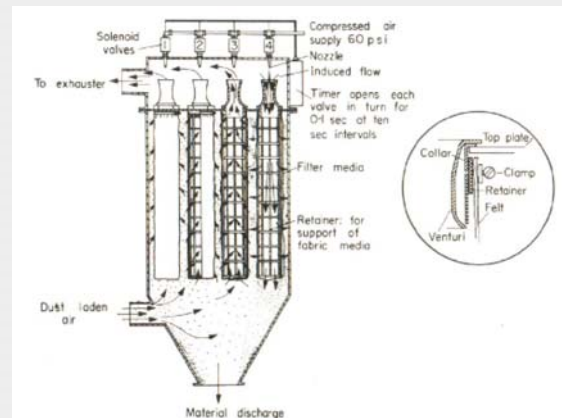
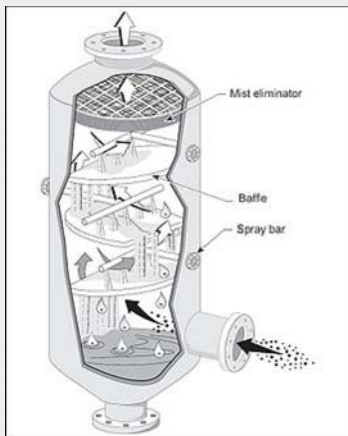
email: cozzolino@irc.cnr.it

**17th ETH Conference on Combustion Generated
Nanoparticles**

Introduction

- ✓ The presence of submicronic particles in flue gases coming from different typology of industrial plants represents a strong concern due to their well known **dangerous effects** on human health and environment.
- ✓ The efficiency of traditional physical **separation processes**, based on diffusion, inertial impact, as well as sedimentation, **in removing** particle with diameters ranging from $0.1 \mu\text{m}$ to $1 \mu\text{m}$ decrease to approximately **25%**, thereby making their application impractical

(<http://www.epa.gov/apti/bces/module3/collect/collect.htm>)



Introduction

- ✓ The presence of submicronic particles in flue gases coming from different typology of industrial plants represents a strong concern due to their well known *dangerous effects* on human health and environment.
- ✓ The efficiency of traditional physical *separation processes*, based on diffusion, inertial impact, as well as sedimentation, *in removing* particle with diameters ranging from 0.1 μm to 1 μm decrease to approximately *25%*, thereby making their application impractical
(<http://www.epa.gov/apti/bces/module3/collect/collect.htm>)
- ✓ A novel technique for both industrial and domestic applications relies on the *diameter increasing* of fine and ultra-fine particles by *condensing water vapor* onto the particles themselves. The great availability of vapor makes this technique interesting for a wide range of industrial processes and combustion facilities.



Potential Applications

High content of vapor present in the flue gases

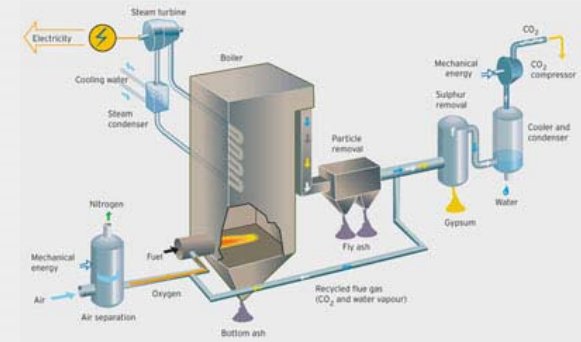
MILD Oxy-Fuel combustion

Vapor Condensational Scrubbing Process

Biomass pyrolysis process

Easy availability of vapor at relatively low temperatures

Chemical, glass, cement metallurgy industry



Primary aim of work

- ✓ Analysis of flue gases cleaning by means activation of heterogeneous water condensation on particles as function of inlet temperature and vapor concentration with particular regard to the effect of their dimension, concentration and chemical nature on temporal evolution and condensational growth activation process.

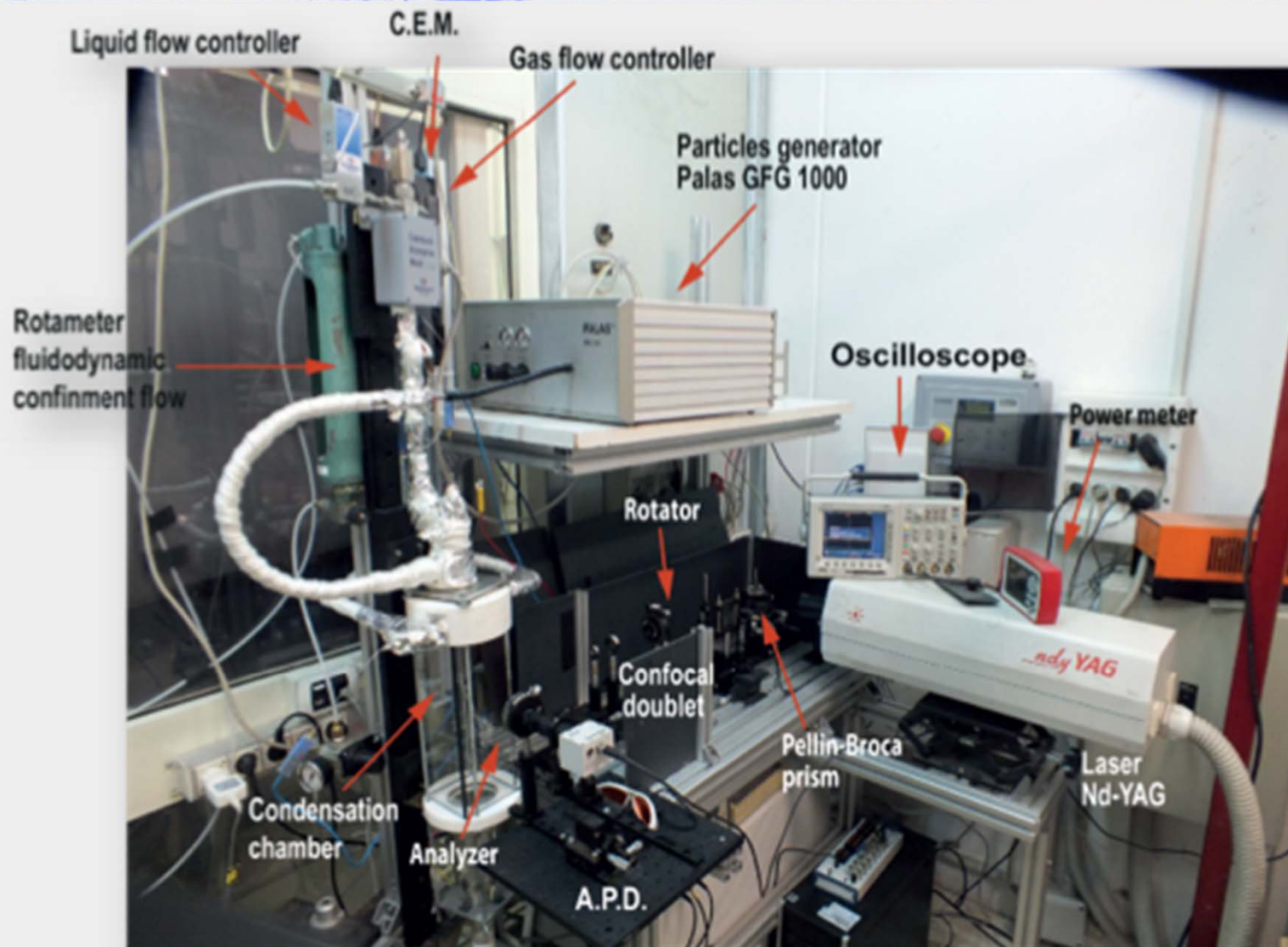


Approach

- ✓ Vapor nucleation on submicronic particles has been experimentally followed in a laminar flow chamber.
- ✓ Characteristic times and the dynamic of the process are experimentally evaluated in dependence on operative conditions and particles characteristics.



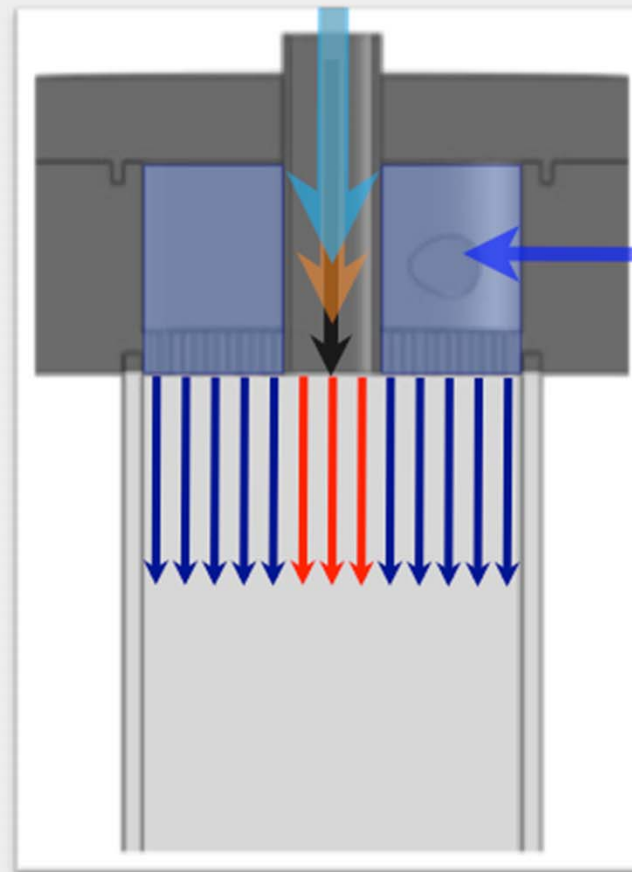
Experimental set-up



Feeding configuration

Main flow
Vapor (H₂O), Carrier (Ar) & Particles (C or Fe or Ni)
(T_{in}, X_v_{in})

- ▶ The working conditions of particle generator ensure a monodispersed particle distribution with the maximum at 150nm (10 nm C only) and with a number concentration of about $2 \cdot 10^7$ #/cm³ ($6 \cdot 10^7$, $1 \cdot 10^8$ #/cm³ C only)
- ▶ Only particles and carrier are fed to the flow chamber at $X_v = 0$
- ▶ Same fluid-dynamic conditions for all operating condition considered
- ▶ Laminar flow



**Confinement
Flow (Air)**
T_c=298 K



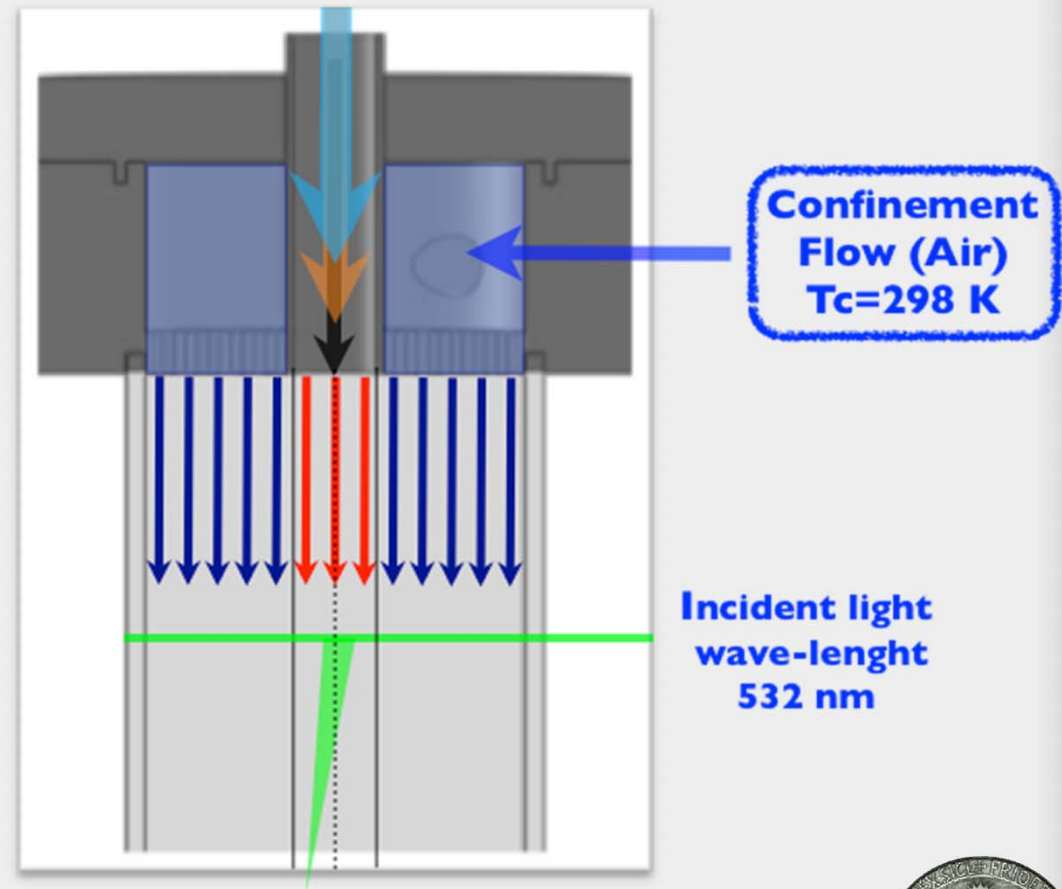
Spatial temporal profile of polaritation ratio

Main flow
Vapor (H_2O), Carrier (Ar) & Particles (C or Fe or Ni)
(T_{in} , Xv_{in})

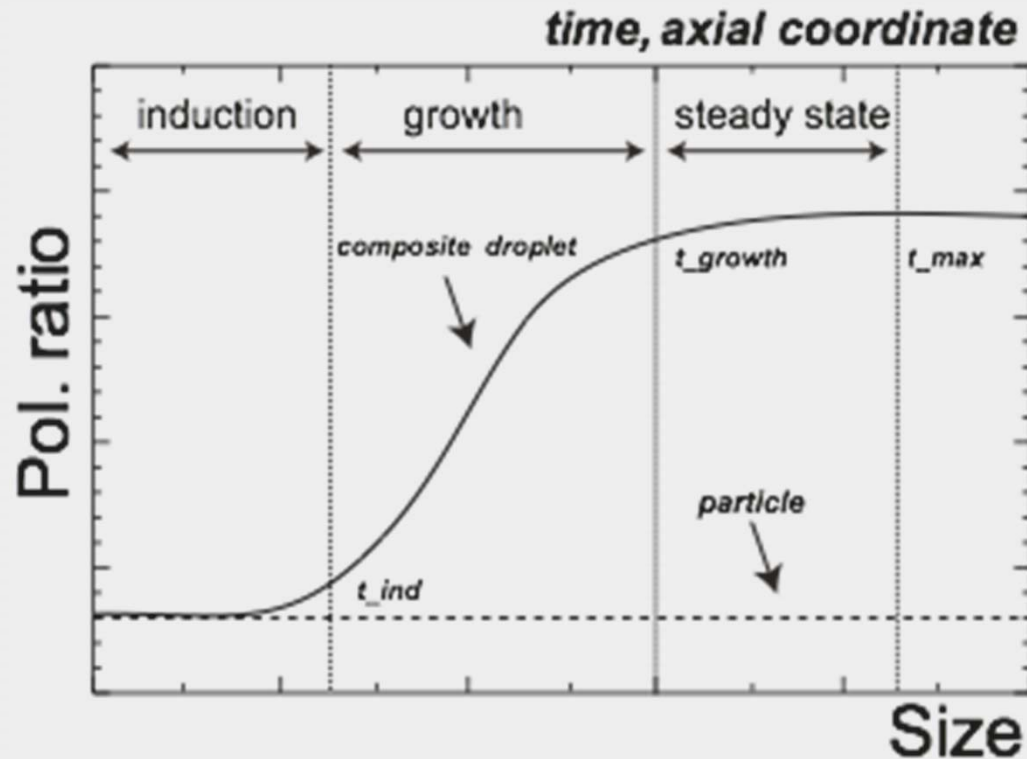
► Intensities of elastically scattered light I_{VV} and I_{HH} were measured along chamber and then polarization ratio

$$\gamma = I_{HH}/I_{VV}$$

was evaluated varying operating conditions and particles characteristics. The evolution of the condensation process can be analysed following the temporal profiles of polarization ratio for the working conditions considered.



Qualitative spatial/temporal evolution of droplet growth process



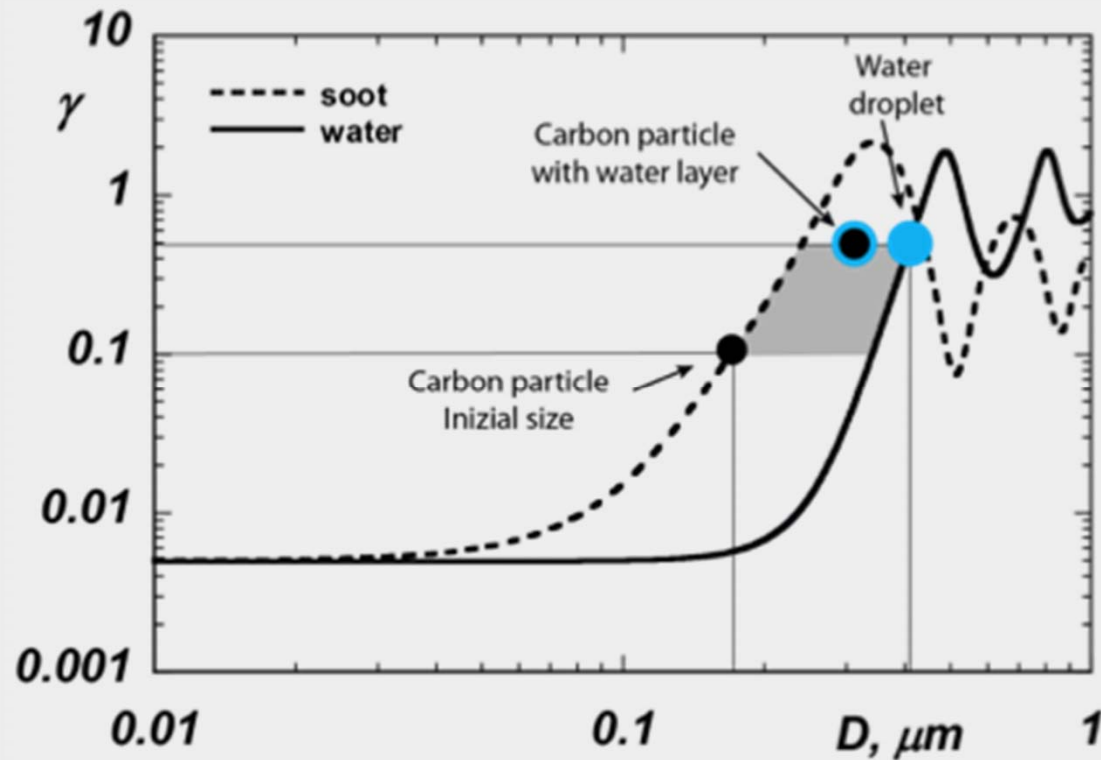
$$\gamma = \gamma(D, m)$$

$$\gamma = I_{HH} / I_{VV}$$

$\gamma \rightarrow 0$ nanoscale
 $\gamma \rightarrow 1$ microscale



Qualitative spatial/temporal evolution of droplet growth process



$$\gamma = \gamma(D, m)$$

$$\gamma = I_{HH} / I_{VV}$$

$\gamma \rightarrow 0$ nanoscale

$\gamma \rightarrow 1$ microscale

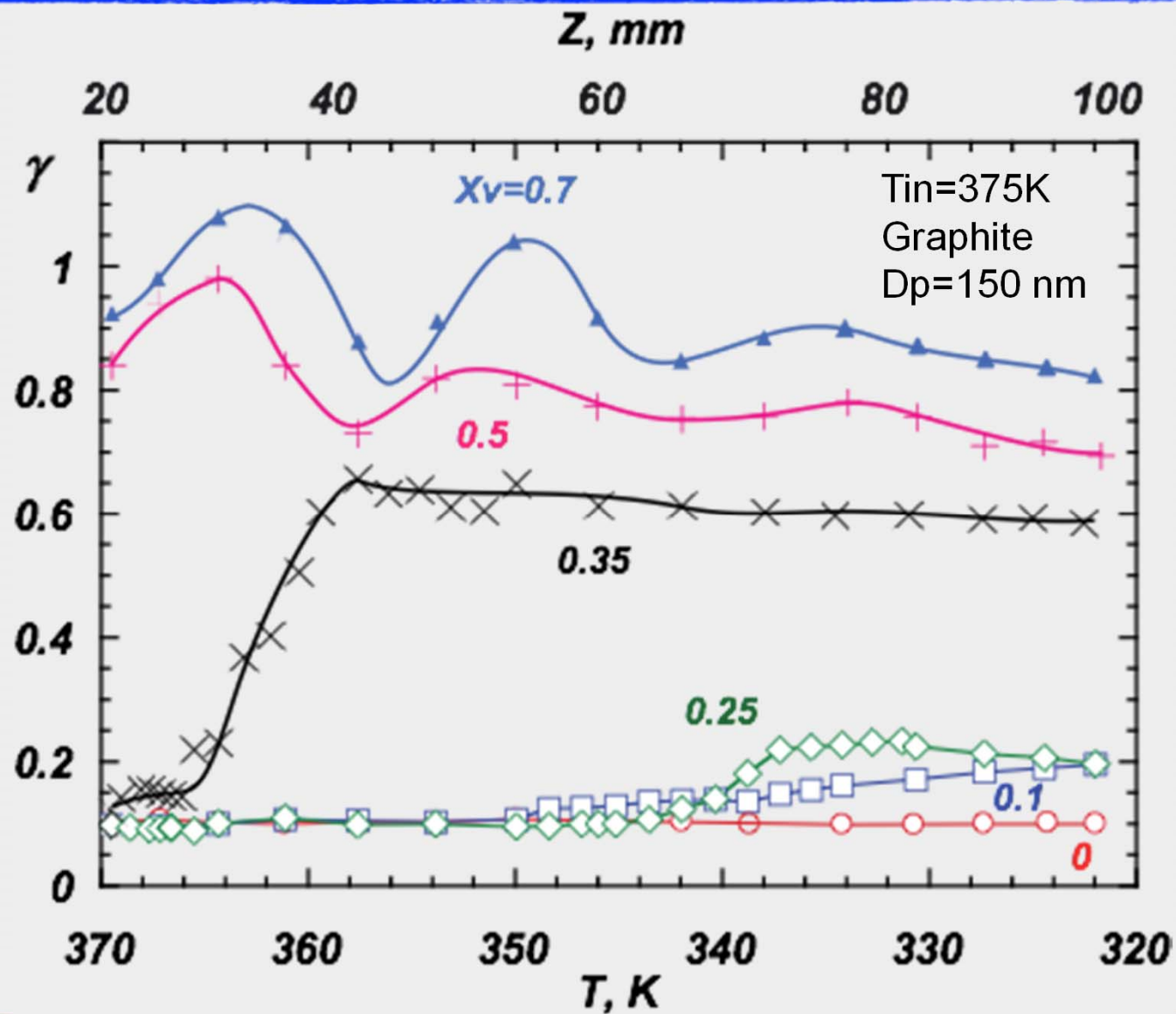


Explored parameter

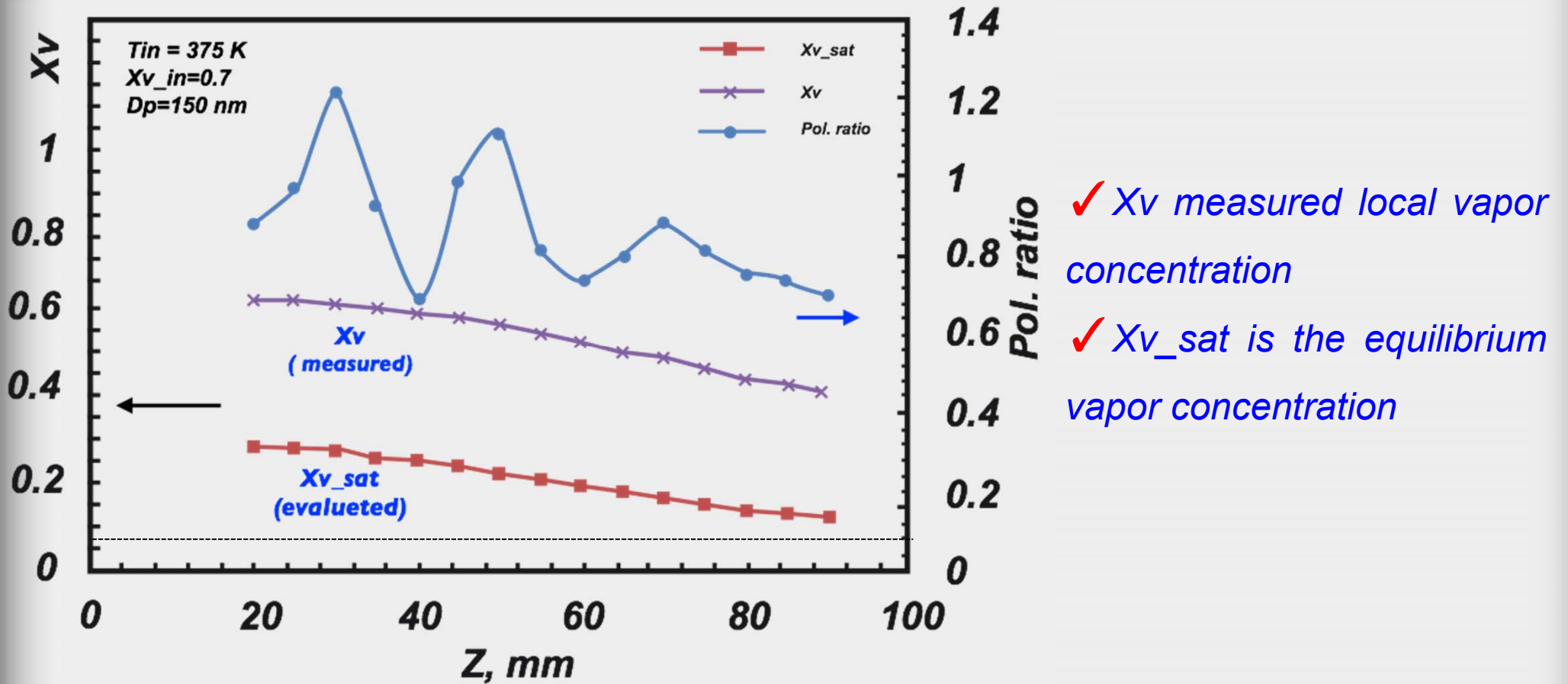
Inlet temperature	T_{in}, K	375 - 405 - 425
Inlet vapor concentration	X_{v_in}	0 - 0.1 - 0.25 - 0.35 - 0.5 - 0.7
Contact angle	$\theta, ^\circ$	20 - 50 - 85
Particles concentration	$N, \#/cm^3$	2.0E+07
Particle Diameter	D_p, nm	150



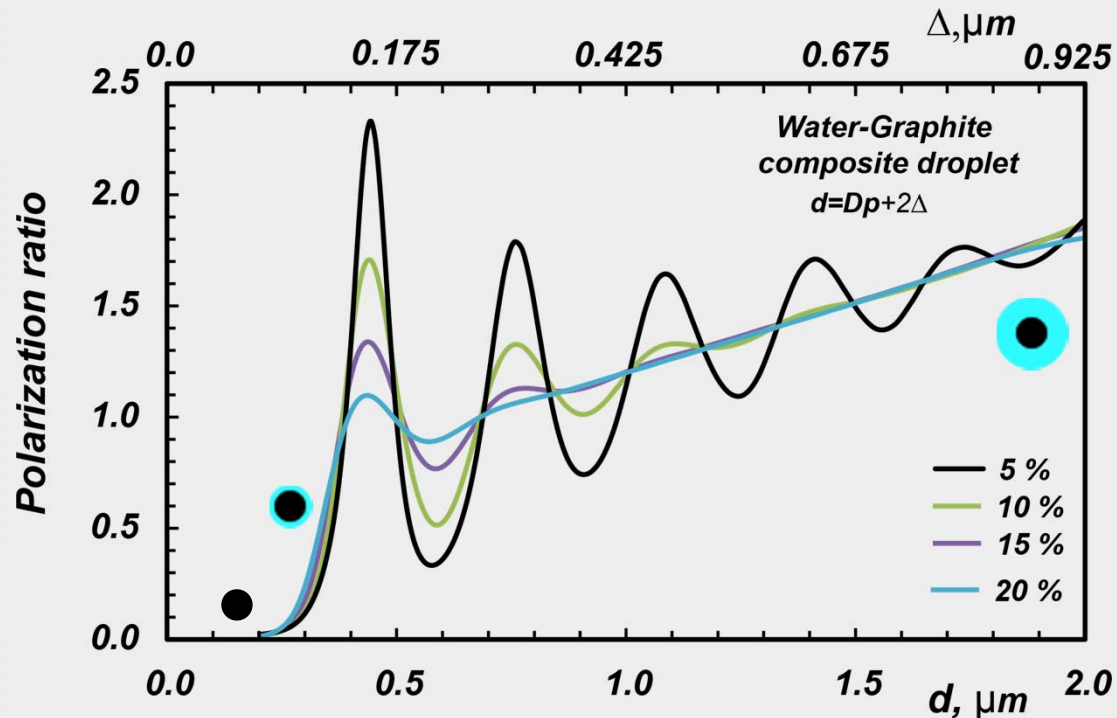
Effect of vapor concentration



Droplet growth



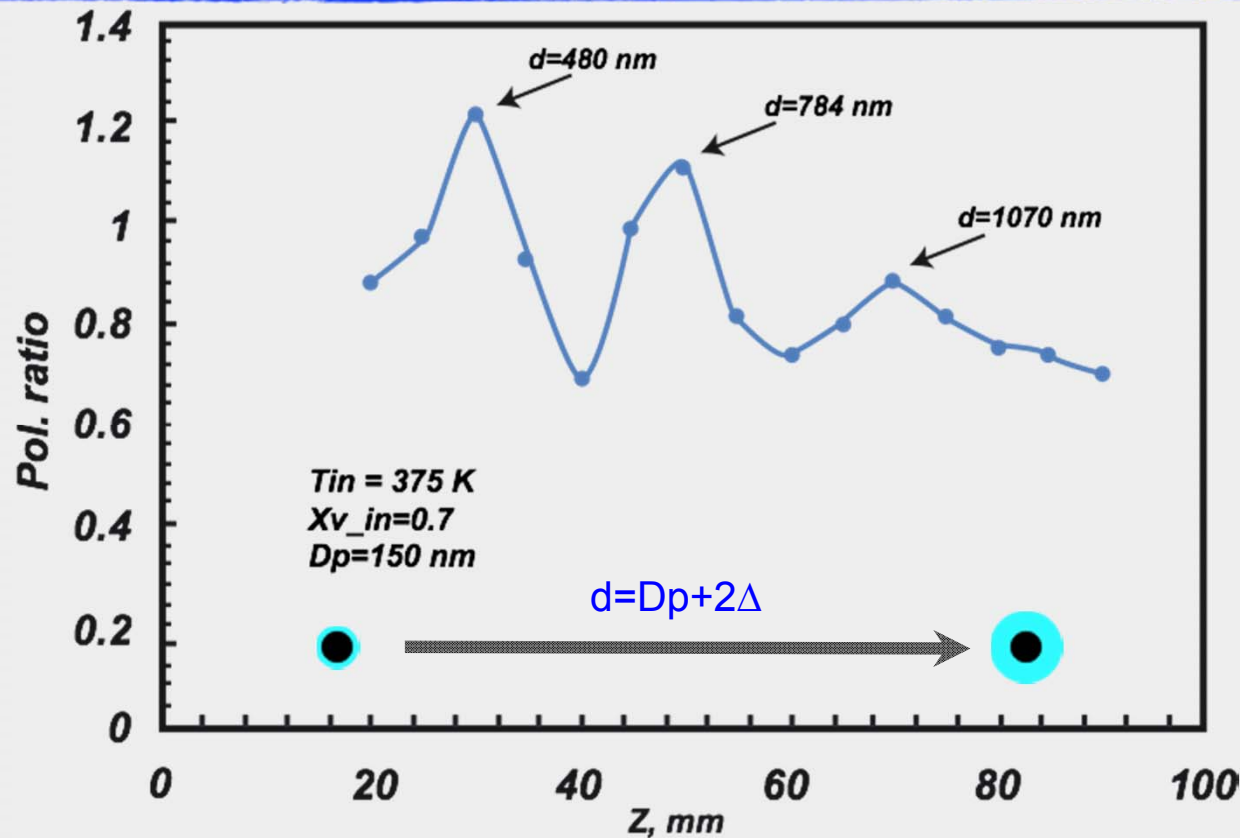
Particle distribution width



- ✓ The observation of **three or more oscillations** in correspondence of the drop size growth.
 - ▶ Maxima in correspondence of well identified droplet sizes
 - ▶ Relatively **narrow size dispersion** of the droplets.
 - ▶ Activation of nucleation and growth **occur contemporaneously on all particles**.



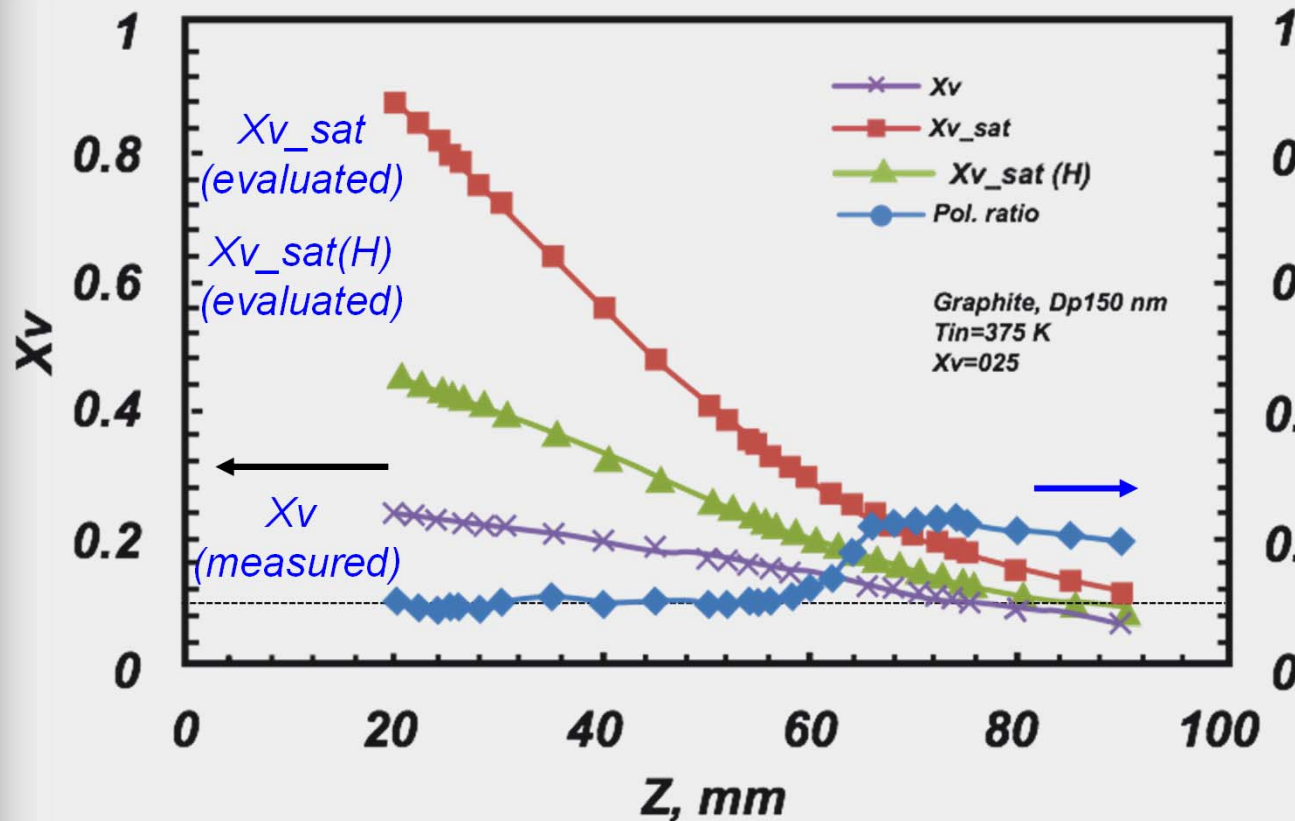
Particle distribution width



- ✓ The observation of **three or more oscillations** in correspondence of the drop size growth.
 - ▶ Maxima in correspondence of well identified droplet sizes
 - ▶ Relatively **narrow size dispersion** of the droplets.
 - ▶ Activation of nucleation and growth **occur contemporaneously on all particles**.



Droplet growth - effect of local conditions



✓ X_v measured local vapor concentration

✓ X_{v_sat} is the equilibrium vapor concentration

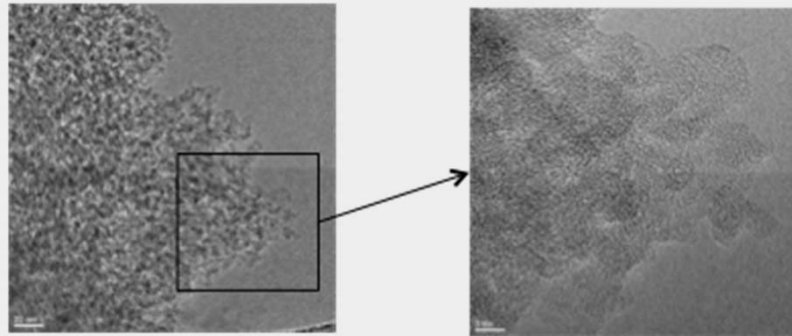
✓ $X_{v_sat}(H)$ strongly depends on surface morphology, chemical and physical properties

H is the mean curvature of liquid meniscus present on interspace between primary particles
 $H < 0$



Chemical-physical particle characterization

Graphite

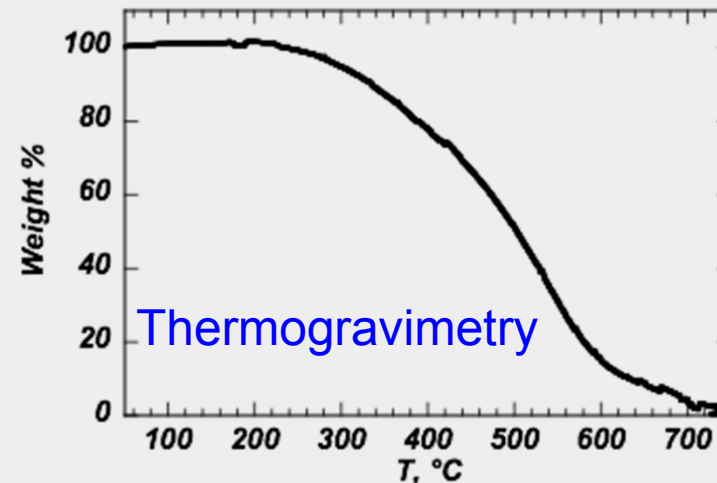
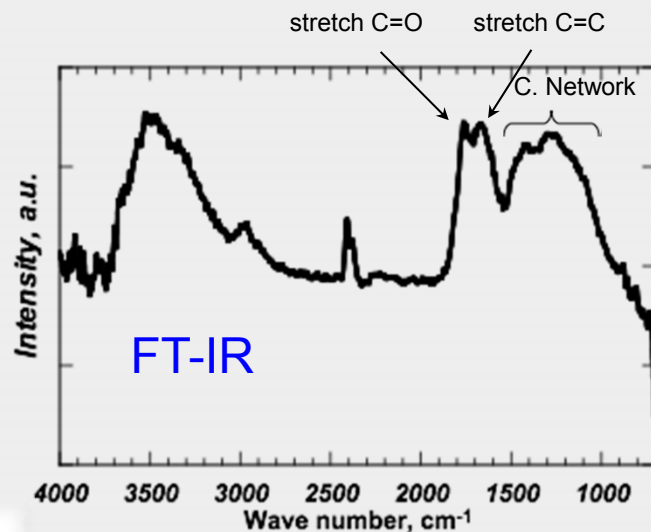


HRTEM: Primary particle size: 3-5 nm

✓ TEM images show that particle surface is far more than spherical and homogeneous FT-IR shows that there are oxygenated functional groups on particle surface

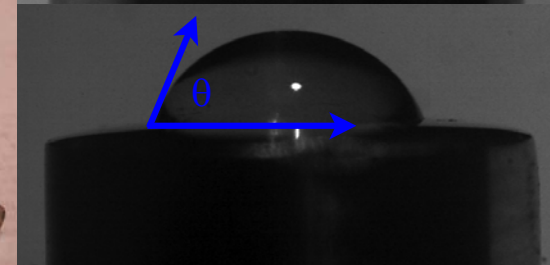
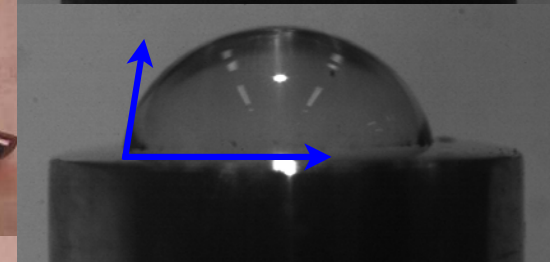
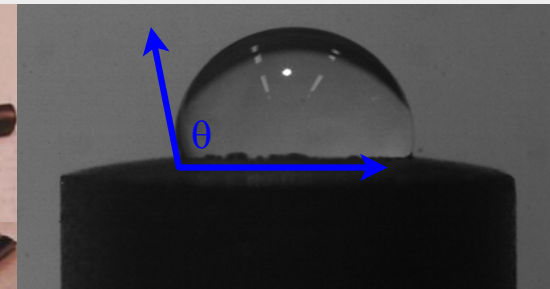
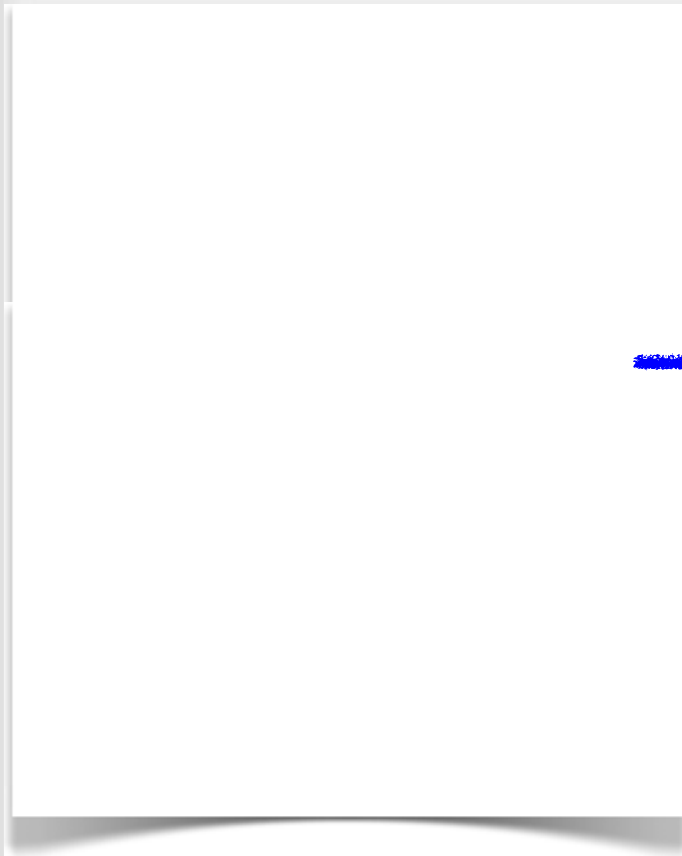
✓ The particle has a microporous network (Specific surface area 310 m²/g) (Kuznetsov et al., 2003)

✓ The morphological and structural properties of the particle justify the onset of certain physical phenomena responsible for particles size growth even at sub-saturation conditions



Particles spark generator

- N , D_p , Chemical species



↑
Contact angle

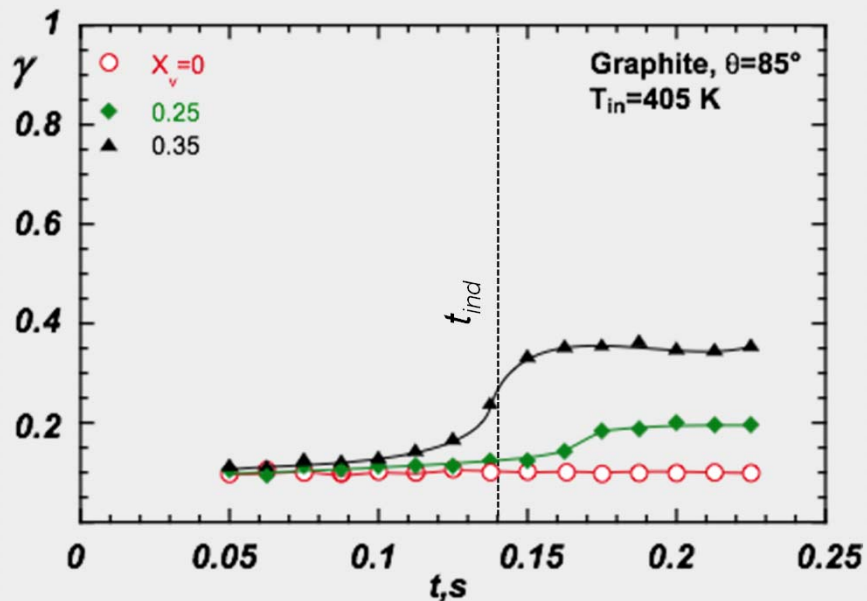
Aerosol production efficiency

Thermal, and electrical conductivity, boiling point, melting point

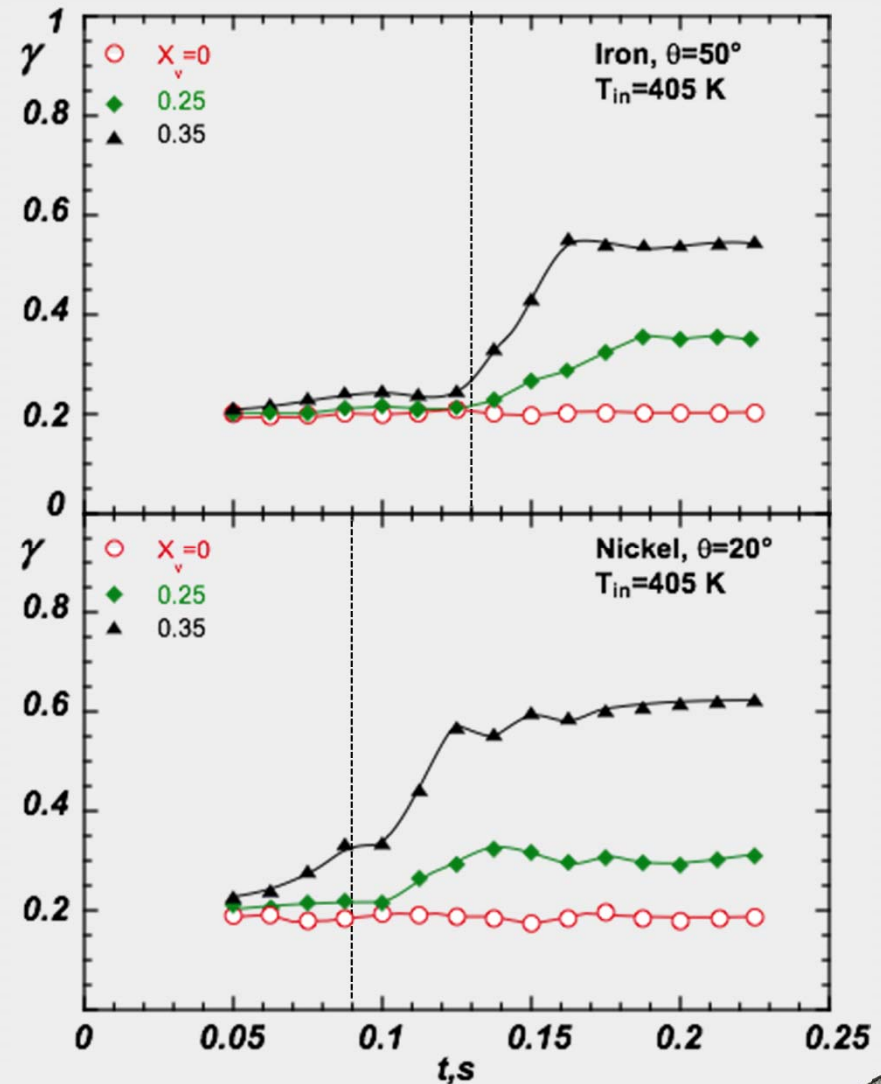


Effect of Particles Chemical Nature

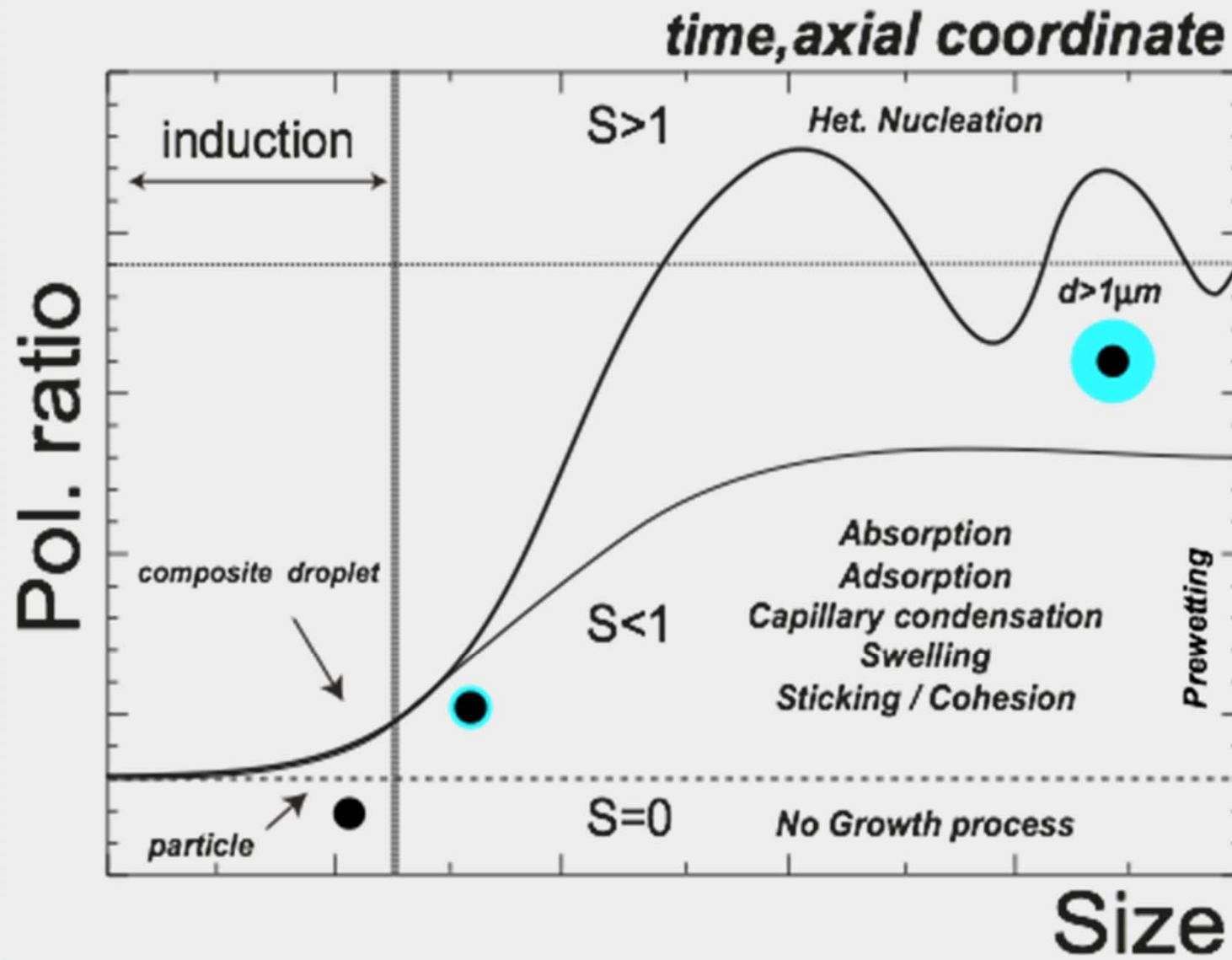
✓ An increase of particle wettability reduces induction and growth time



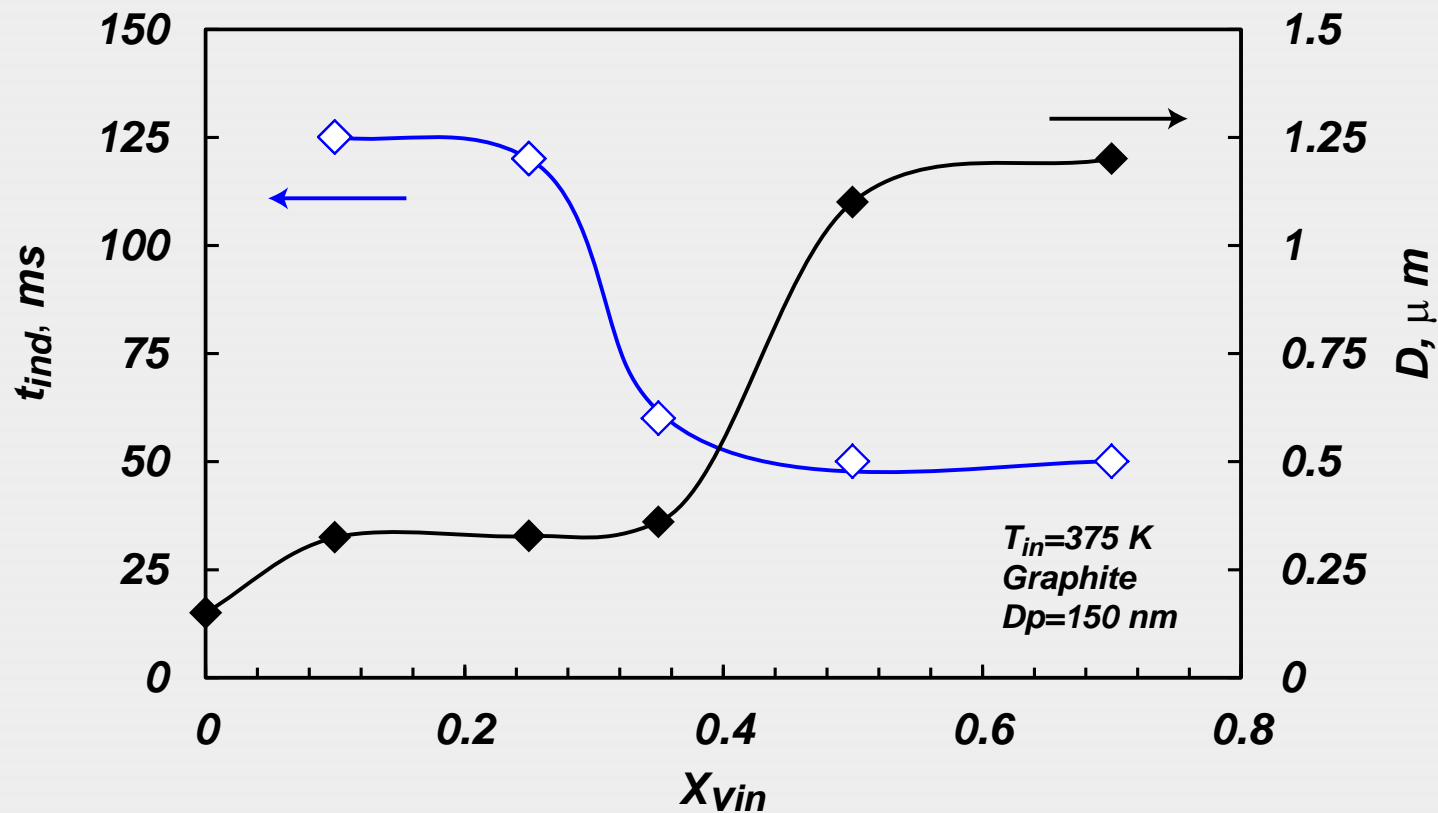
✓ A stronger interaction between particle and condensed vapor species improves water uptake



Qualitative pol. ratio trends : Scheme of interpretation



Final droplet size & Induction time



- ▶ High inlet vapor concentration and low working temperature :
 - ▶ Final size of the particles increases
 - ▶ Induction time of process decreases



Main Conclusions

- Two particle growth mechanisms, involving different physical processes:
 - ✓ Saturation < 1 :
 - Particle covering related to its morphology and chemical-physical properties.
 - Size variation relatively low
 - ✓ Saturation > 1:
 - Particle covering driven by vapor concentration
 - Final size of the droplet of the order of microns
- Efficiency:
 - ✓ Both mechanisms particularly efficient for particles capture
 - ✓ Unitary efficiency with respect to particle activation



General Conclusions

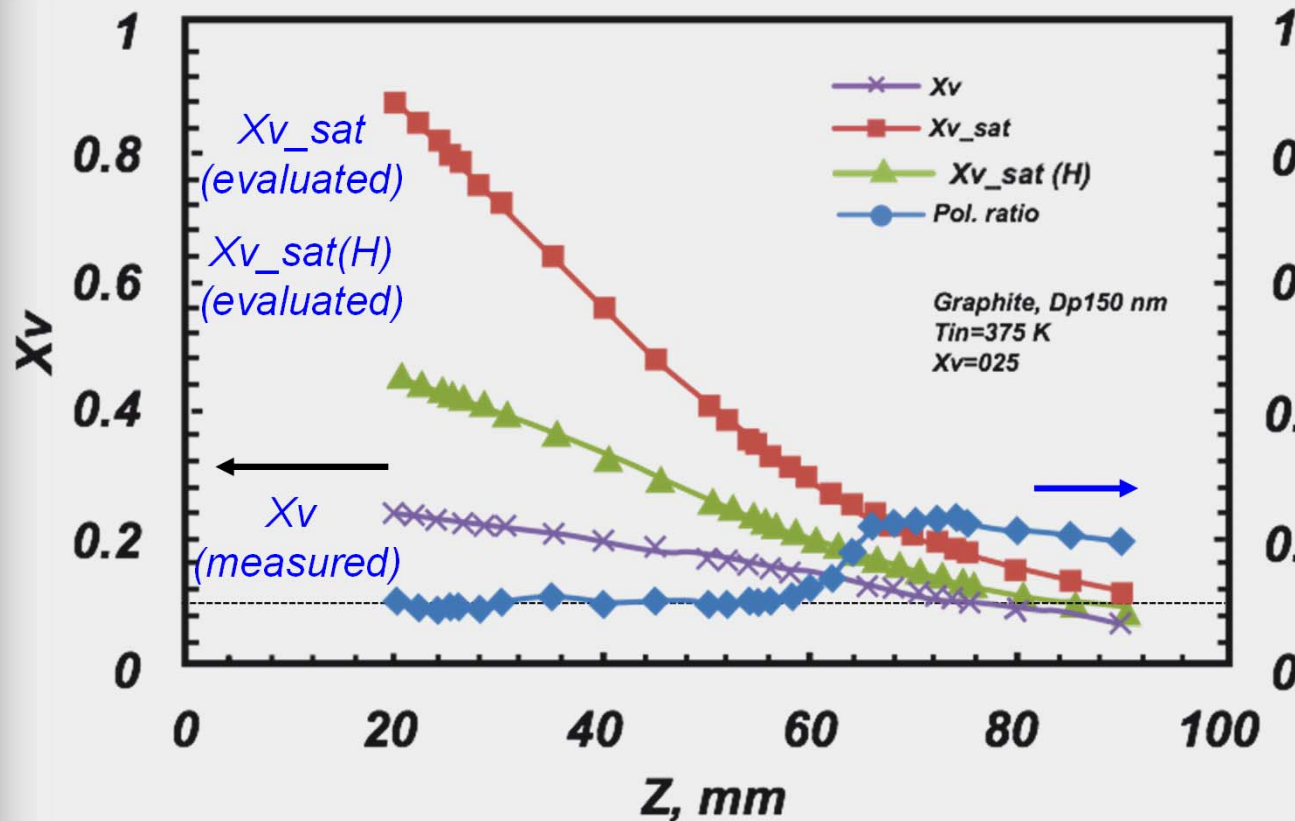
- ✓ *The induction and growth times experimentally evaluated, are compatible with practical applications and useful for the design of a real abatement unit.*
- ✓ *The optimal operating condition of the process depends on the quality of the flue gas stream to be treated*
- ✓ *Potentially extreme working conditions can be very useful for the particle covering. In fact, these processes are active also at relatively low vapor concentration.*
- ✓ *From practical point of view also such a limited dimension of condensed layer is crucial in determining the capture efficiency. In fact, the liquid layer can strongly improves the cohesion/sticking between particles, leading to an overall particle dimension increase.*



Thanks for the attention...



Droplet growth - effect of local conditions



- ✓ X_v measured local vapor concentration
- ✓ X_{v_sat} is the equilibrium vapor concentration
- ✓ $X_{v_sat}(H)$ strongly depends on surface morphology, chemical and physical properties

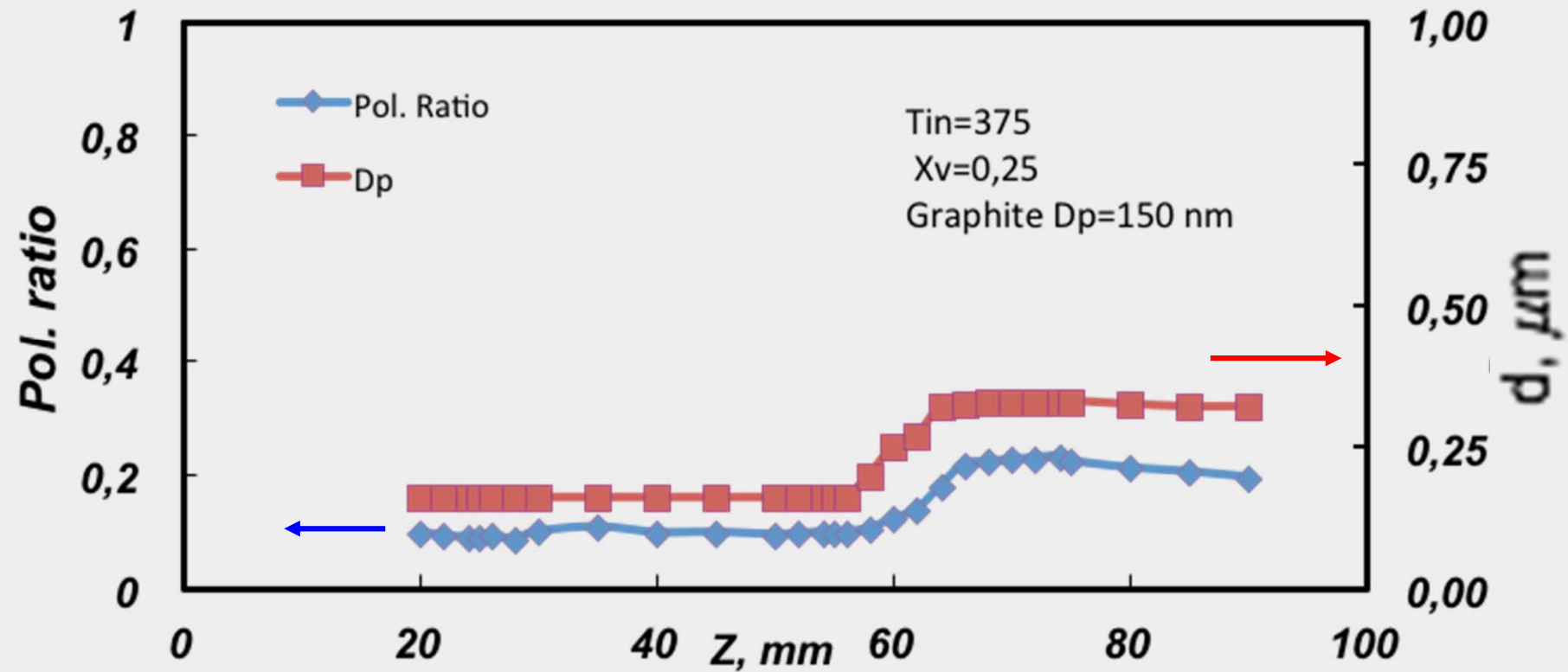
$$P_{sat} = P^\circ(T)$$

$$P_H = P^\circ \exp\left(\frac{M_w \sigma_{lv}}{\rho_l RT} H\right) \rightarrow X_{v_sat}(H)$$

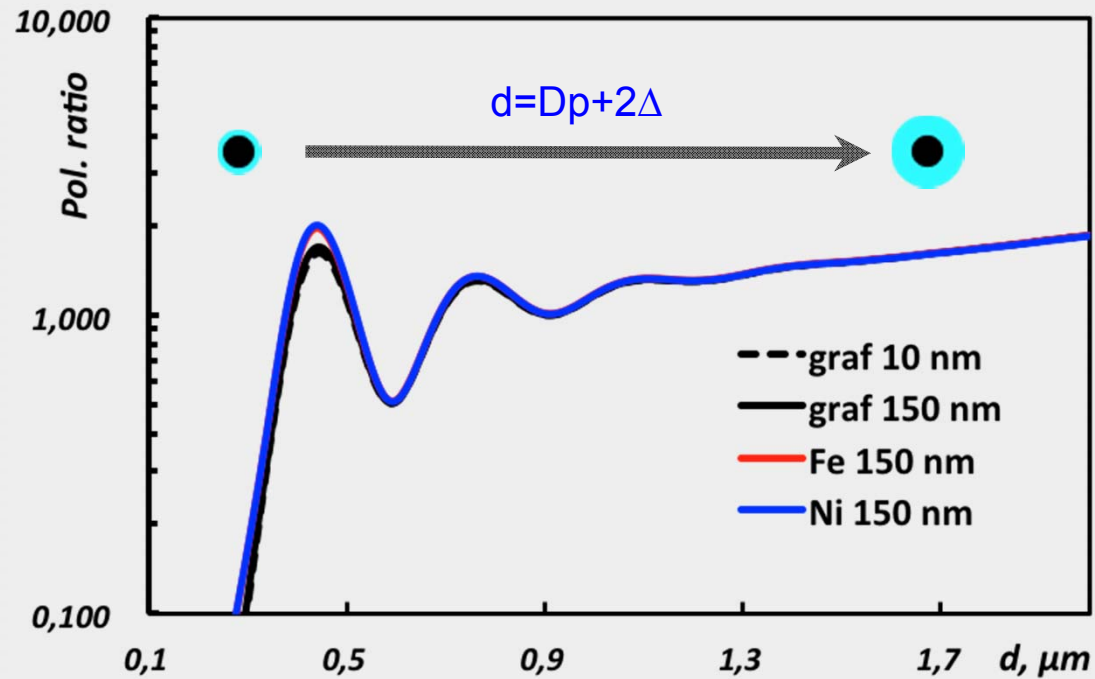
H is the mean curvature of liquid meniscus present on interspace between primary particles
 $H < 0$



Droplet growth



Numerical evaluation of polarization ratio

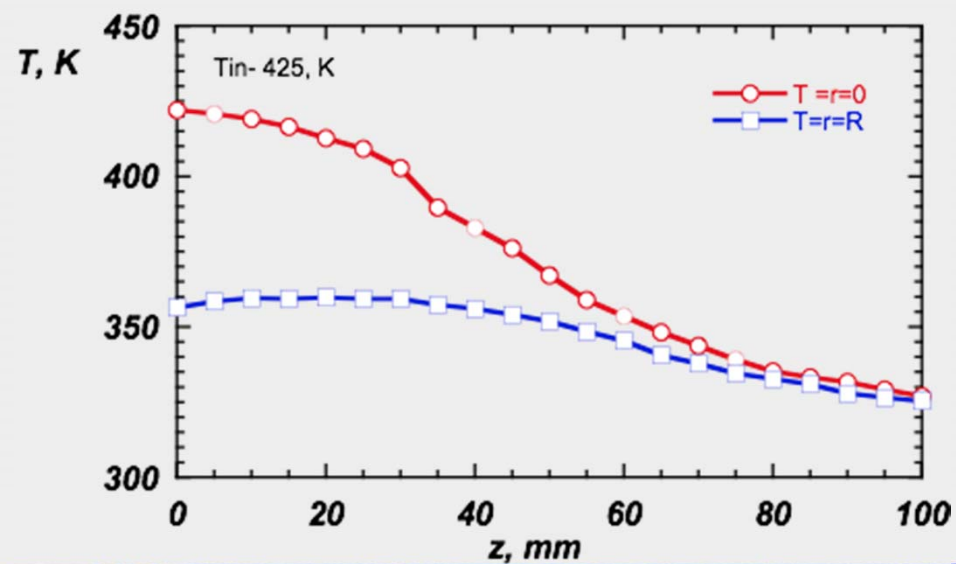
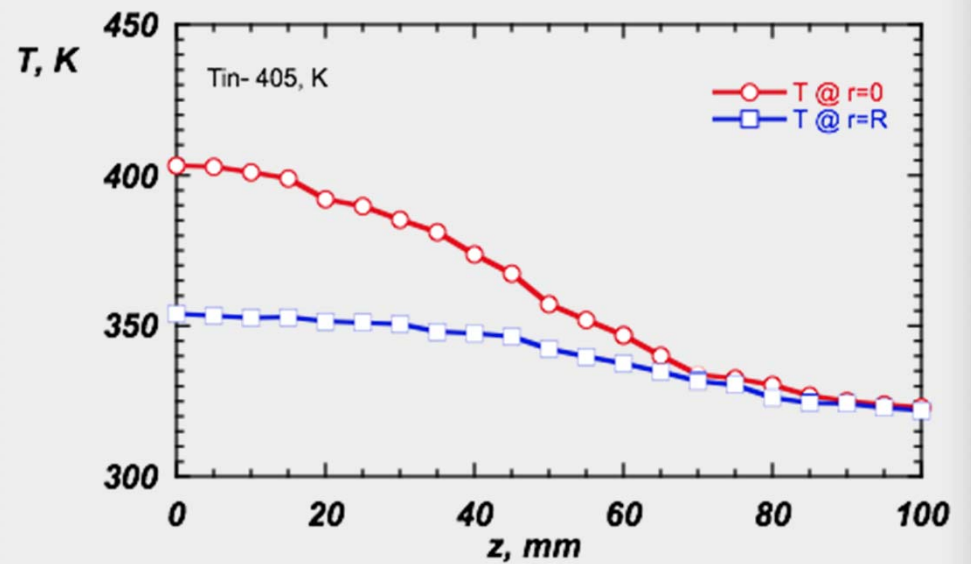
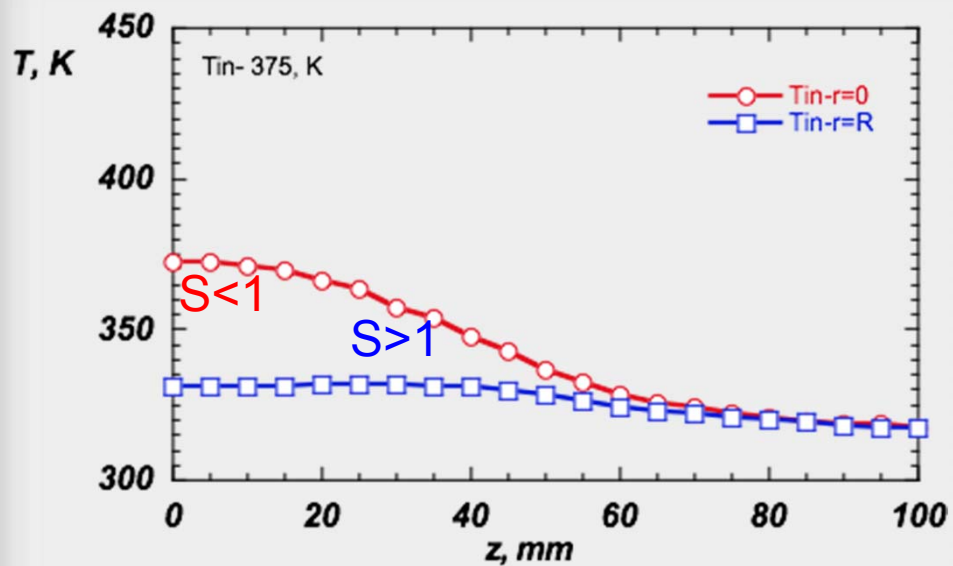


✓ Polarization ratio is independent of the optical properties and size of the particle included in the water shell

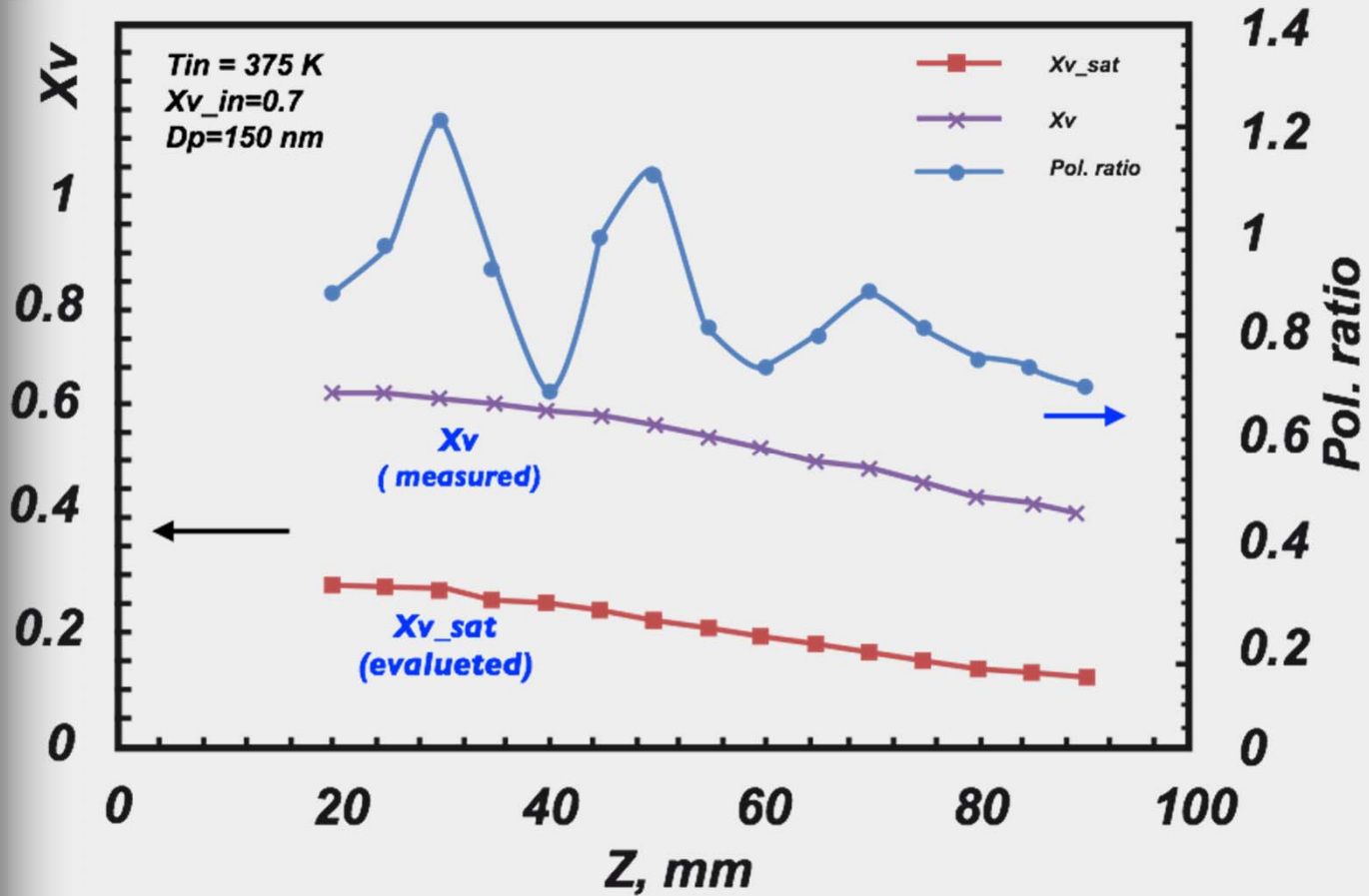
(Gorden Videen and Petr Chylek, 1998)



Temperature Profiles



Droplet growth



Mixing degree

$$\Phi(T) = \frac{T - T_c}{T_{in} - T_c}$$

Local vapor concentration

$$X_v = \Phi(T) \cdot X_{v_in}$$

Local equilibrium vapor concentration

$$P_{sat} = P^\circ(T) \rightarrow X_{v_sat}$$



General consideration

Nucleation is the process in which microscopic fragments of a new phase begin to form:

- ✓ *Homogeneous nucleation*: occurs within pure substance.
- ✓ *Heterogeneous nucleation*: occurs in presence of small foreign aerosol (particles molecules, ions, salts, powders, condensed particles)

HOMOGENEOUS



HETEROGENEOUS



Theoretical remarks

✓ *homogeneous nucleation rate* J is defined as the number of nuclei formed per unit time, is given by a general expression of the type:

$$J = K \exp(-\Delta G)$$

$K = K(T, P, A_k)$: collisional frequency factor

$\Delta G = \Delta G(T, S = P/P^\circ, \text{chemical species})$: free energy barrier

✓ *heterogeneous nucleation rate* J^* is defined as the number of nuclei formed per unit time per particle of radius R_p ($A_p = 4\pi R_p^2$), it is given by:

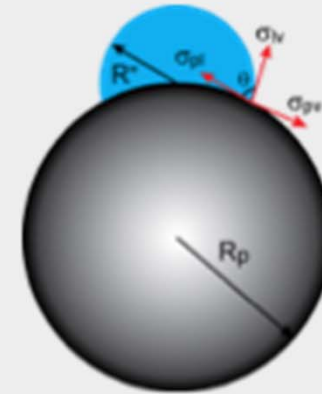
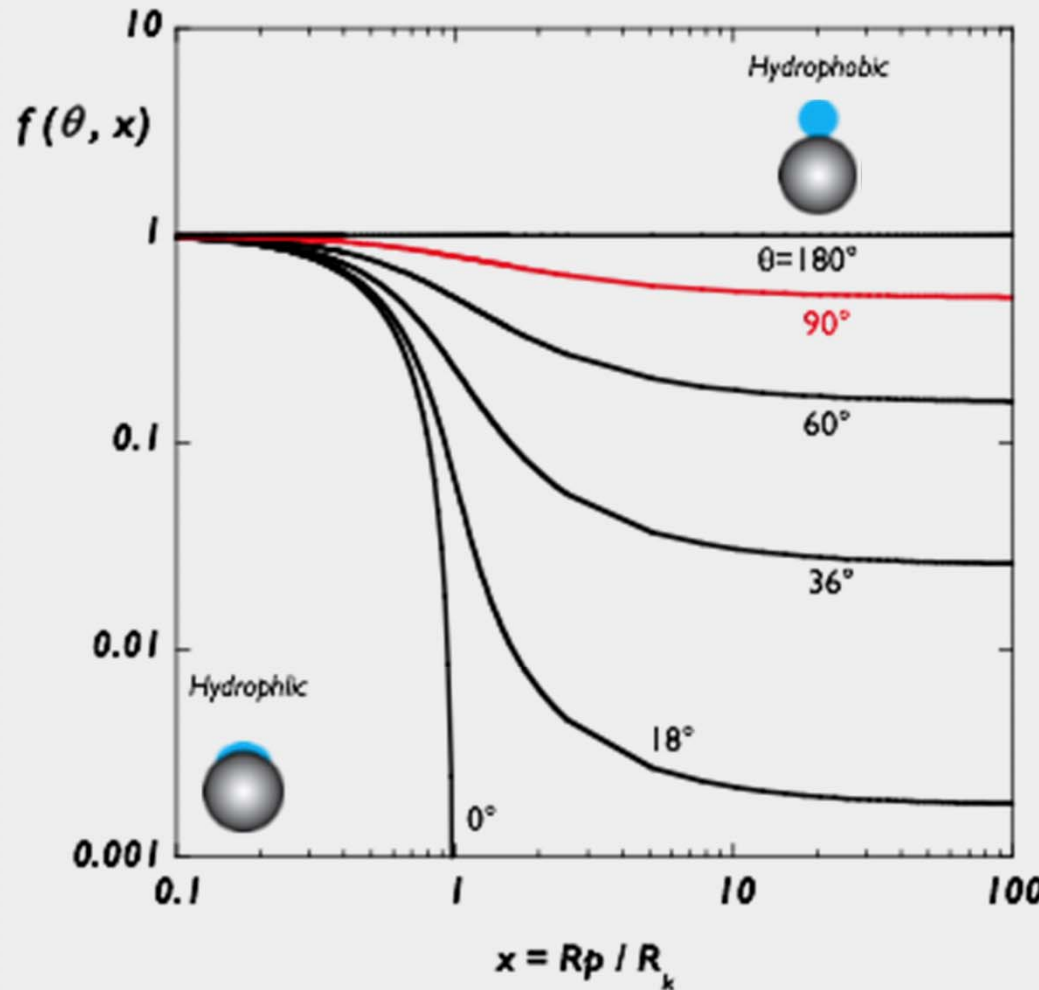
$$J = K^* \exp(-\Delta G^*)$$

$K^* = K^*(T, P, A_p)$; $\Delta G^* = \Delta G \cdot f(\theta, x)$; $\Delta G^* \leq \Delta G$

Heterogeneous nucleation is always thermodynamically favored with respect to homogeneous nucleation.



Free energy barrier reduction factor



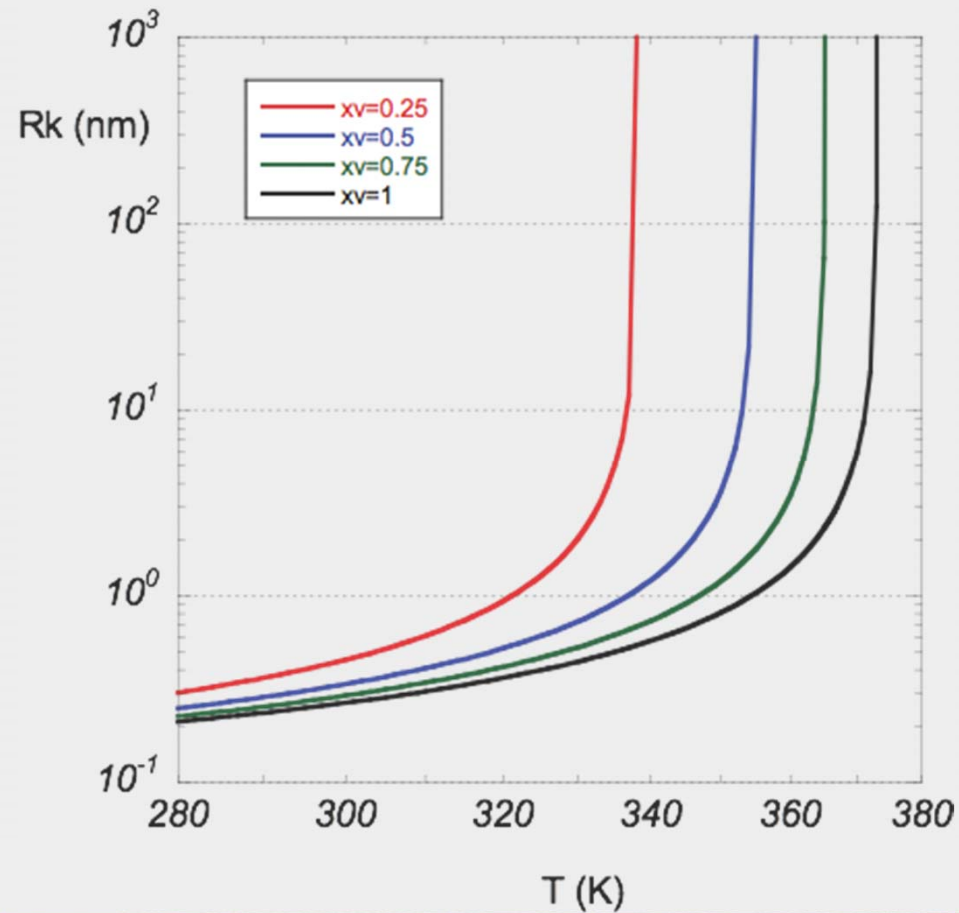
✓ θ is the contact angle between particle and the condensed vapor phase it is also a function of particle surface morphology: $\cos \theta = (\sigma_{pv} - \sigma_{pl}) / \sigma_{lv}$

✓ σ_{pv} , σ_{pl} , σ_{lv} are respectively the free interface energy between: particle-vapor, particle-liquid, and liquid-vapor

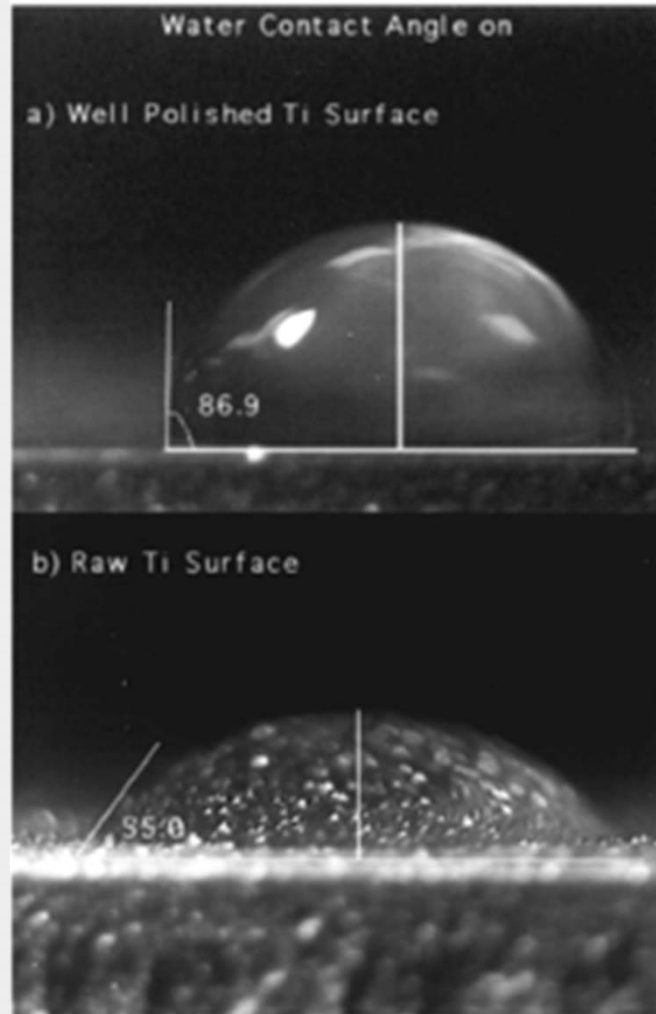
✓ Relative size of foreign particles $x = R_p / R_k$ Kelvin radius (R_k) represents the minimum embryo radius of condensed phase that can be considered stable and suitable for the growth

Kelvin Radius

$$R_k = \frac{2\sigma_{LV}}{n_L k_B T \ln(p_v / p_v^\circ)}$$



Effect of surface roughness



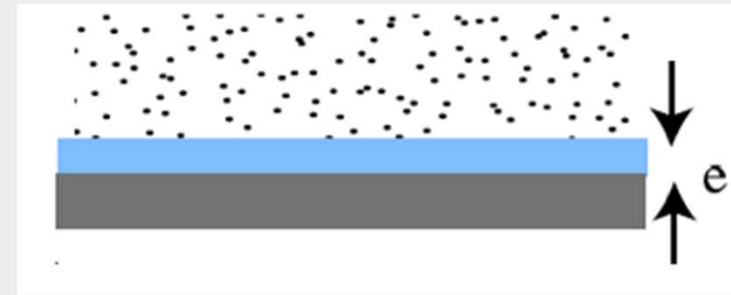
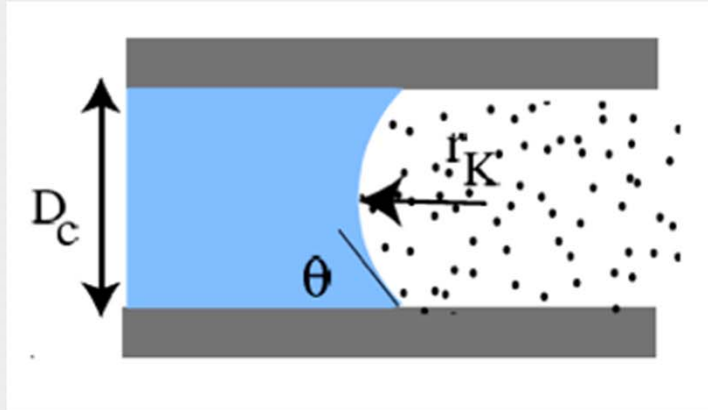
Nucleation rates

(Hering, 2005)	$J = \sqrt{\frac{m_L \sigma_{LV}}{2\pi}} \cdot \left(\frac{p_v}{k_B T}\right)^2 \cdot \frac{2}{\rho_L} \cdot \exp\left\{-\frac{\pi \sigma_{LV}}{3k_B T} d_p^2\right\}$
(Chukanov, 2007)	$J = \sqrt{\frac{2\sigma_{LV}}{\pi m_L}} \cdot \left(\frac{p_v}{k_B T}\right)^2 \cdot \frac{1}{S} \cdot \frac{m_L}{\rho_L} \exp\left\{-\frac{16\pi}{3} \left(\frac{\sigma_{LV}}{k_B T}\right)^3 \left(\frac{m_L}{\rho_L \cdot \ln S}\right)^2\right\}$
(Kotzick, 1996)	$J \square 4\pi a^2 10^{25} \cdot \exp\left\{-\frac{16\pi \sigma_{LV}^3 m_L^2}{3k_B T (\rho_L R T \cdot \ln S)^2}\right\}$
(Kumala et al., 1992)	$J = n_s^2 \cdot s \cdot v_L \sqrt{\frac{2\sigma_{LV}}{\pi m_L}} \cdot \exp\left\{\theta - \frac{4\theta^3}{27 \log^2(S)}\right\} \quad \theta = \frac{s\sigma_{LV}}{k_B T}$
(Kashichiev, 2006)	$J = \frac{A}{16B^4} \cdot \exp\left(\frac{3B^{1/3}}{4^{1.3}}\right) \cdot \ln(S)^{12m} \cdot S \cdot \exp\left\{-\frac{B}{(\ln S)^{2m}}\right\} \quad \Lambda = \frac{M}{\rho_L N_A} \sqrt{\frac{2\sigma_{LV}}{\pi M}} \left(\frac{p_v}{k_B T}\right)^2 \quad B = \frac{16\pi v_L^2 \sigma_{LV}^3}{3(k_B T)^3}$
(Frenkel, 1955)	$J_{Fr} = \frac{(\rho_v \xi_v)^2}{\rho_L m_L} \cdot \sqrt{\frac{2\sigma_{LV}}{\pi m_L}} \cdot \exp\left\{-\frac{\pi \sigma_{LV} d_p^2}{3k_B T}\right\}$
(Becker, Döring, 1935)	$J_{BD} = (g^*)^{-2/3} \cdot J_{Fr} \quad g^* \cong n \cdot \exp\left(-\frac{\Delta G^*}{k_B T}\right)$
(Girshick et al., 1990)	$J_{Gi} = \frac{1}{S} \cdot \exp\left(\frac{\sqrt{36\pi v_L^2 \sigma_{LV}}}{k_B T}\right) \cdot J_{Fr}$

$$J = K \exp(-\Delta G)$$

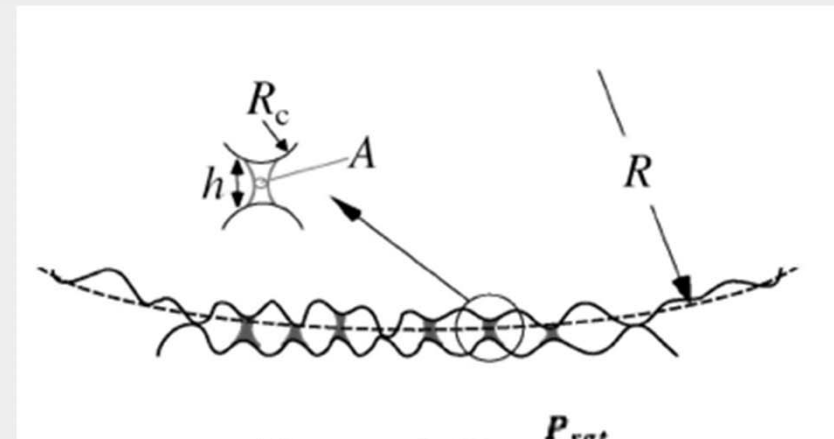
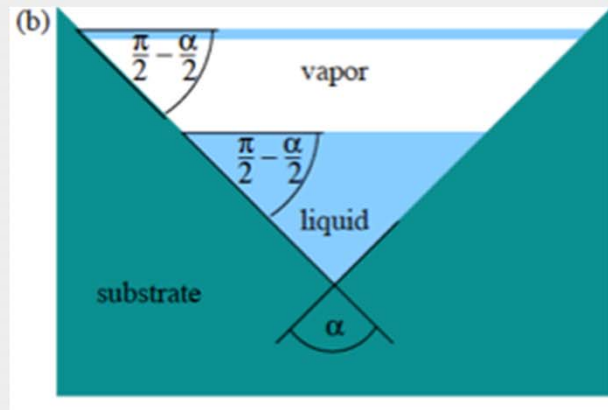


Theoretical remarks



$\theta \rightarrow 0^\circ$

$$D_c(\mu) = \frac{2\sigma_{lv}\cos\theta}{\Delta\mu} = 2r_K\cos\theta$$

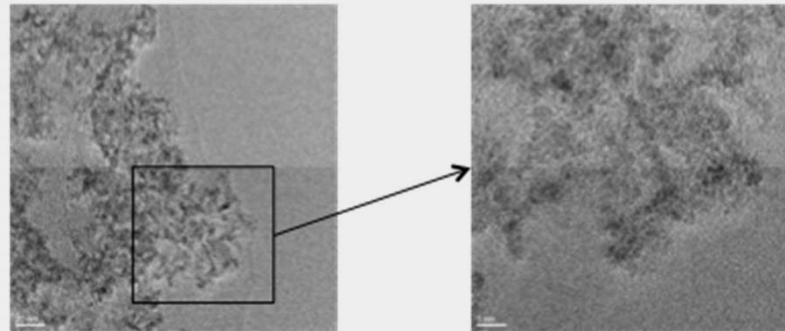


$$\Delta G = v_d \rho_l k_B T \log \frac{P_{sat}}{P_v}$$

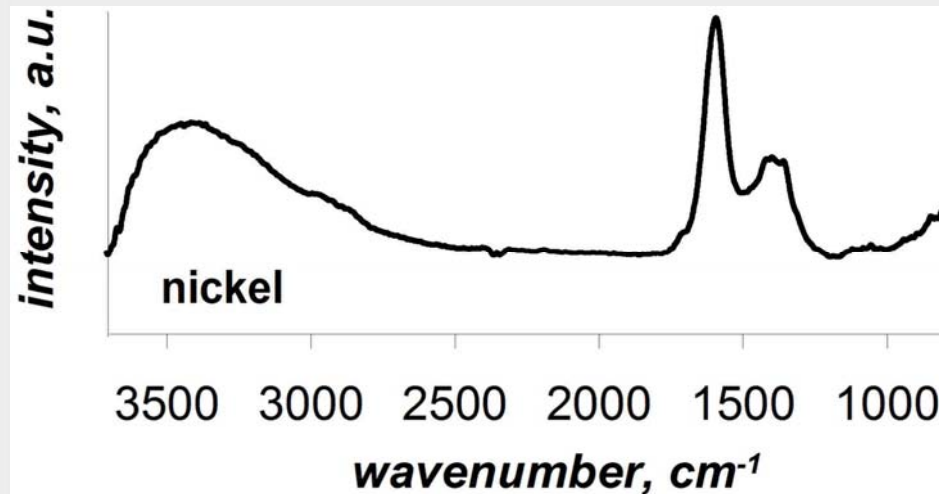


Chemical-physical particle characterization

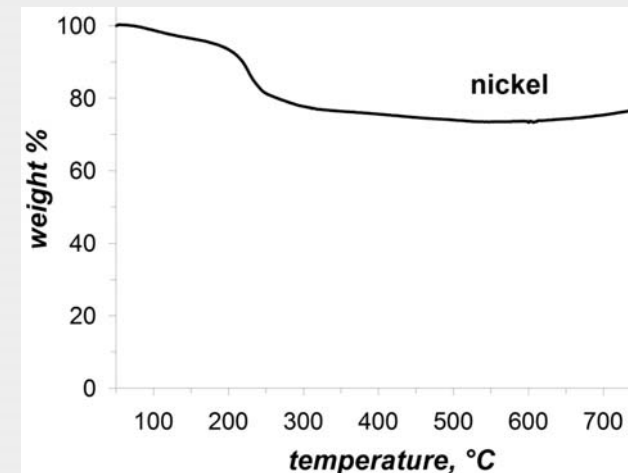
Nickel



HRTEM: Primary particle size: 2-3 nm



FT-IR

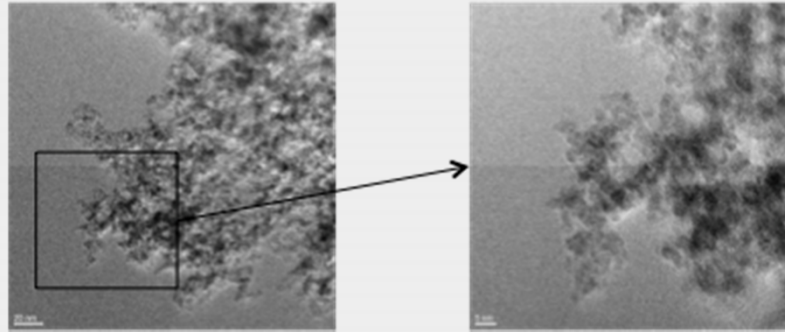


Thermogravimetry

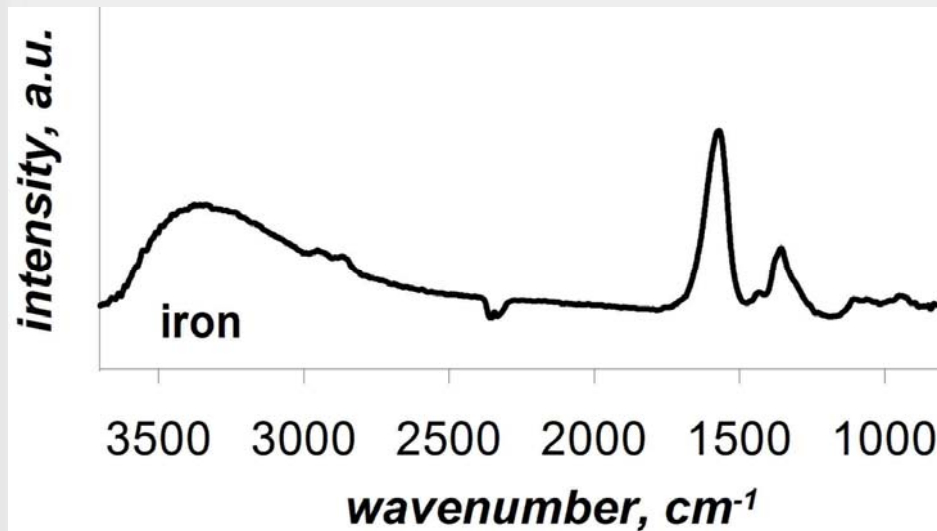


Chemical-physical particle characterization

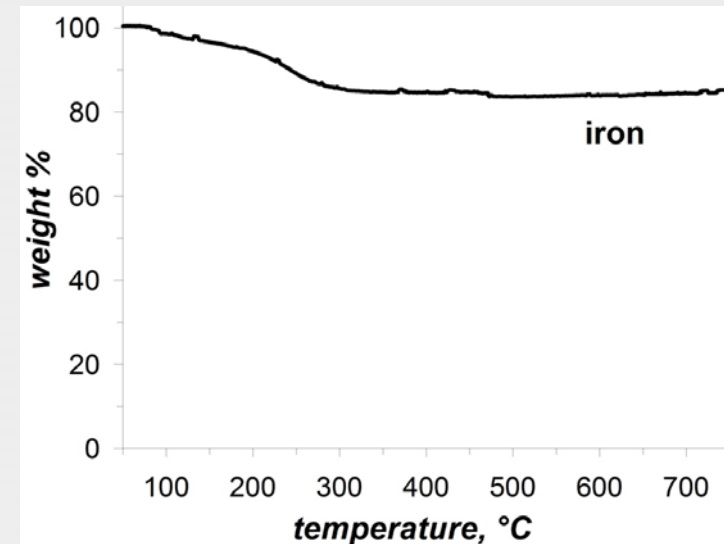
Iron



HRTEM: Primary particle size: 1-2 nm



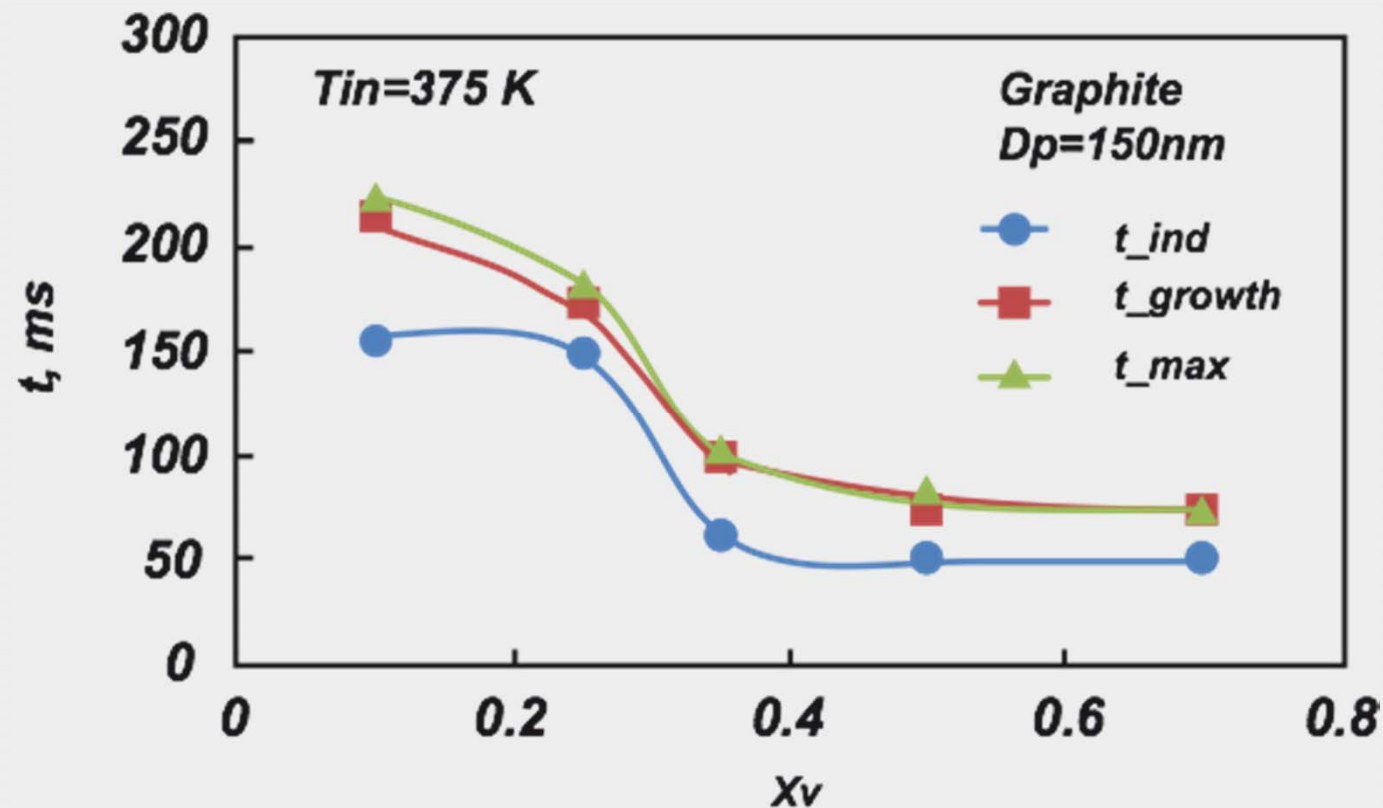
FT-IR



Thermogravimetry



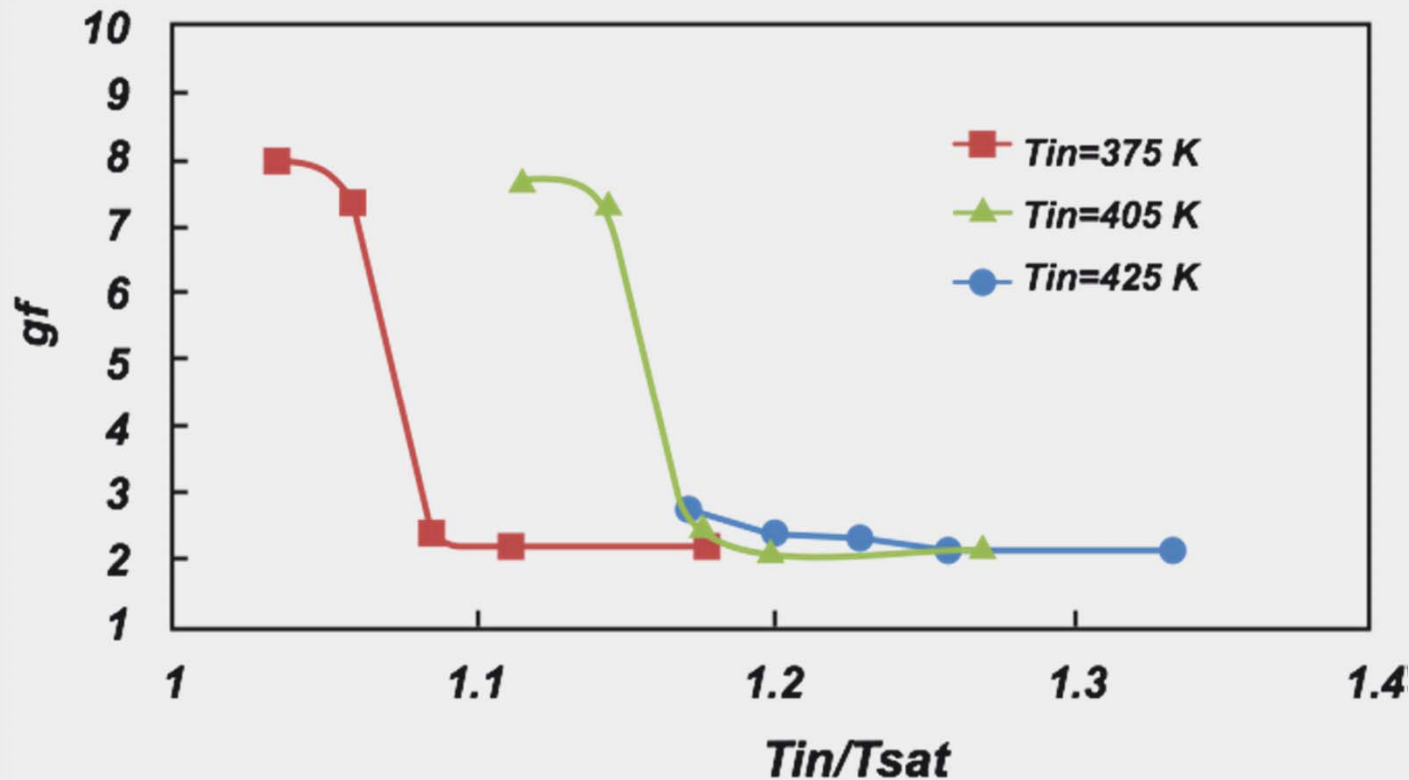
Characteristic times



- ✓ The induction and growth times experimentally evaluated, are compatible with practical applications.
 - Same considerations for all operating conditions considered



Growth Factor

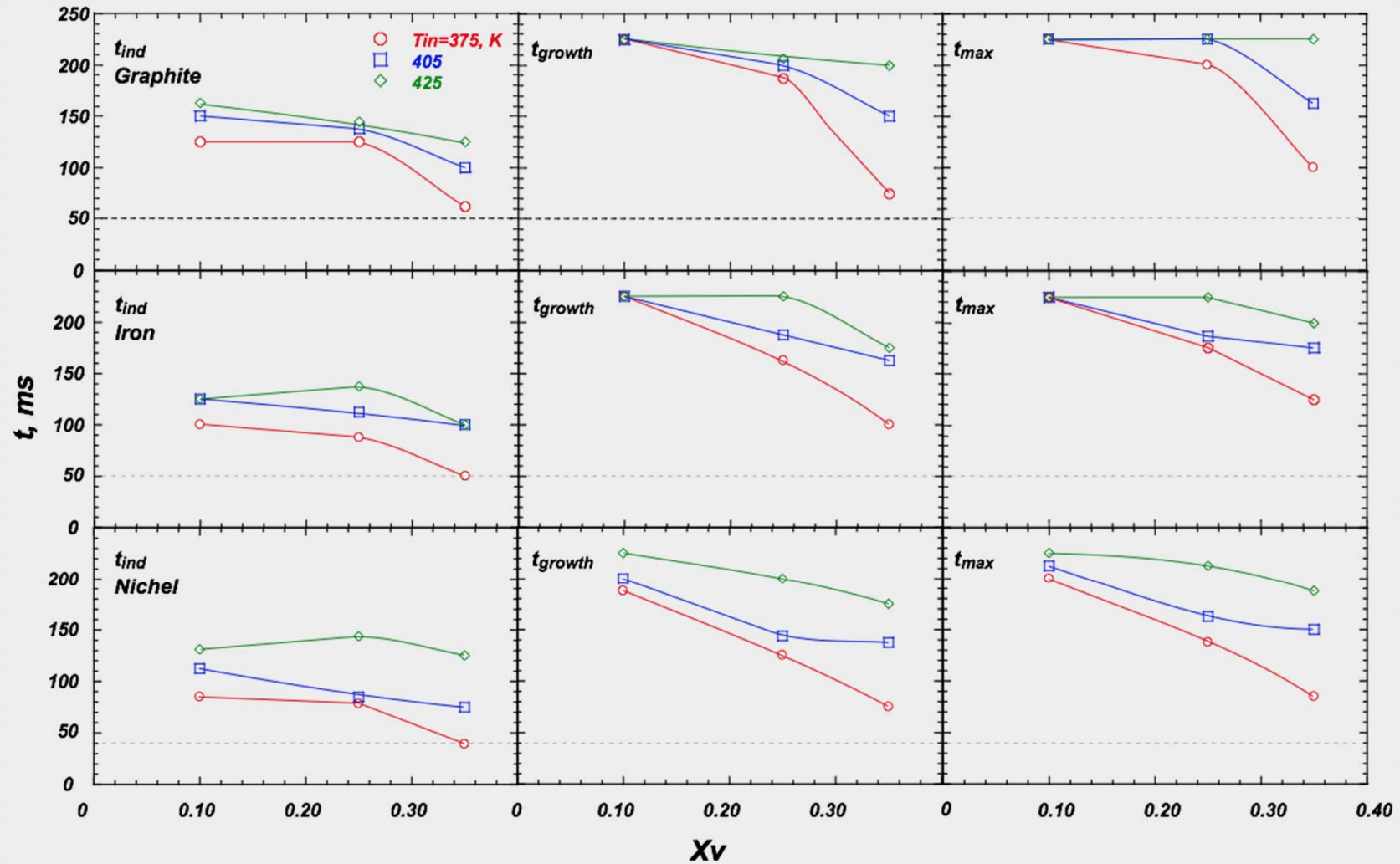


$$g_f = \frac{d}{D_p}$$

✓ The growth factor is the ratio between the final size of droplet and initial size of solid particle.

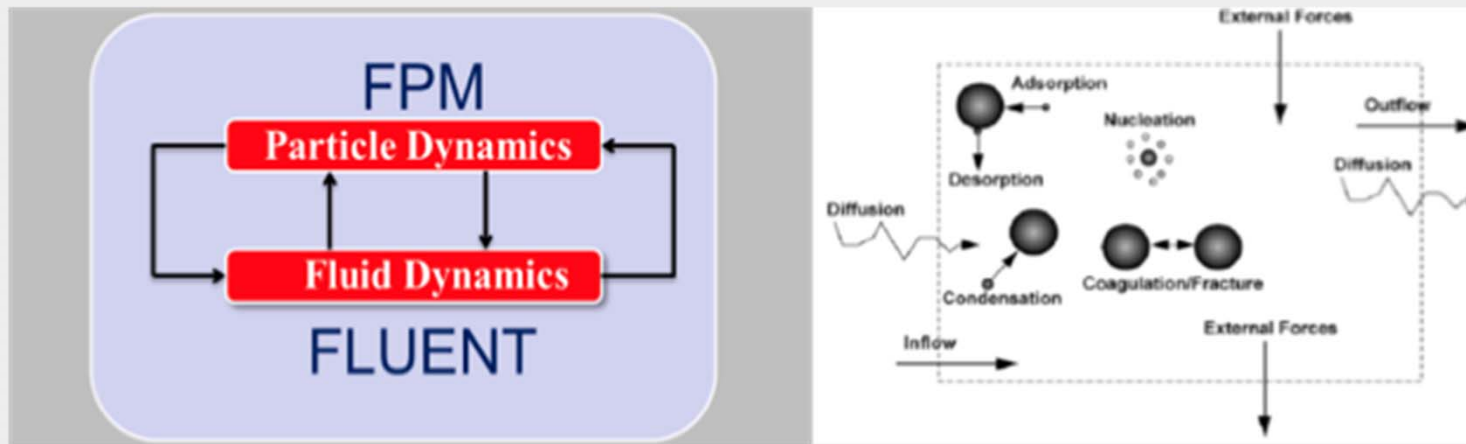


Characteristic times



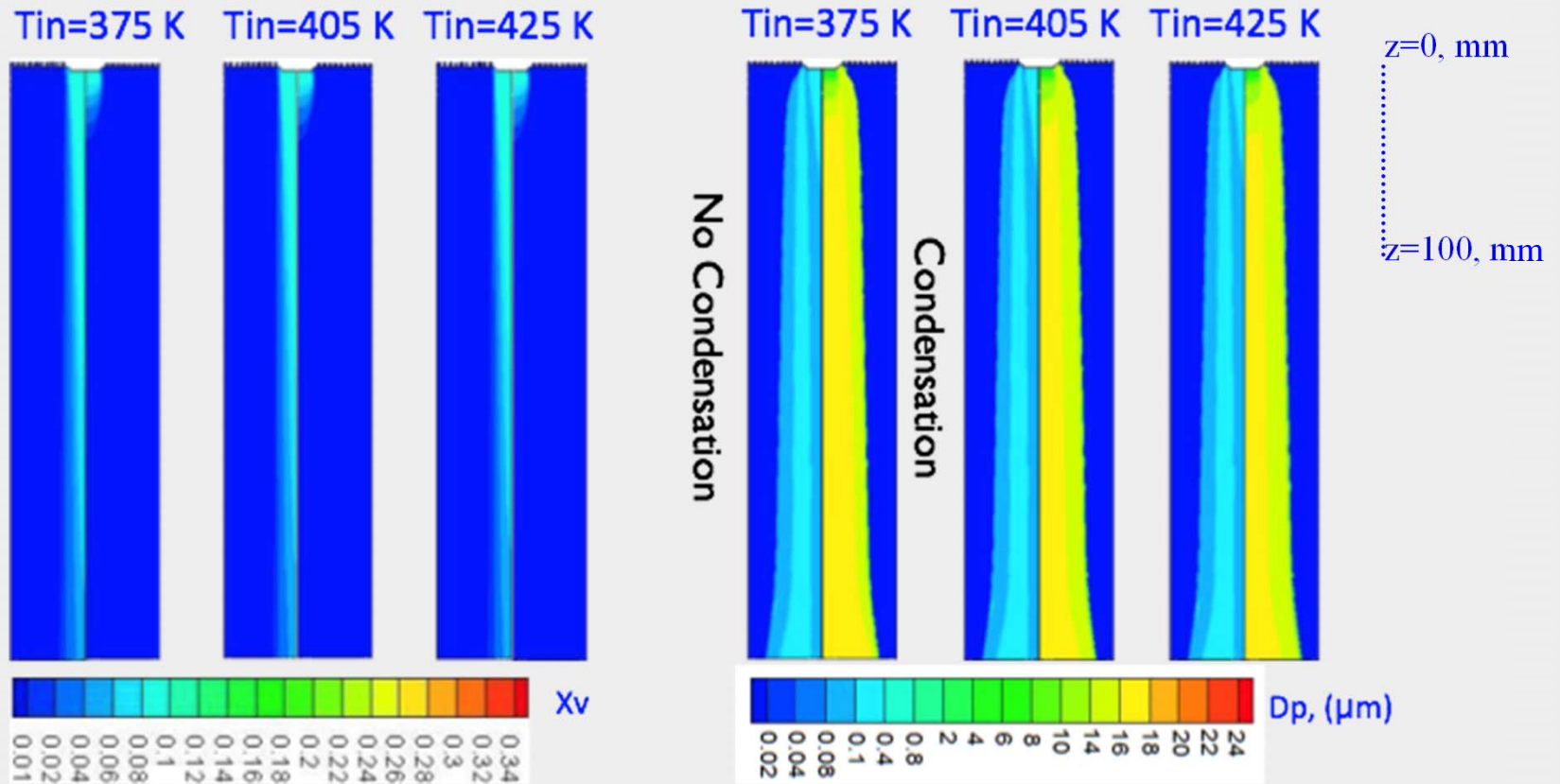
Numerical Tools

During the design of chamber, some numerical simulation on fluid dynamic field and on condensation process, has been carried out by using FLUENT

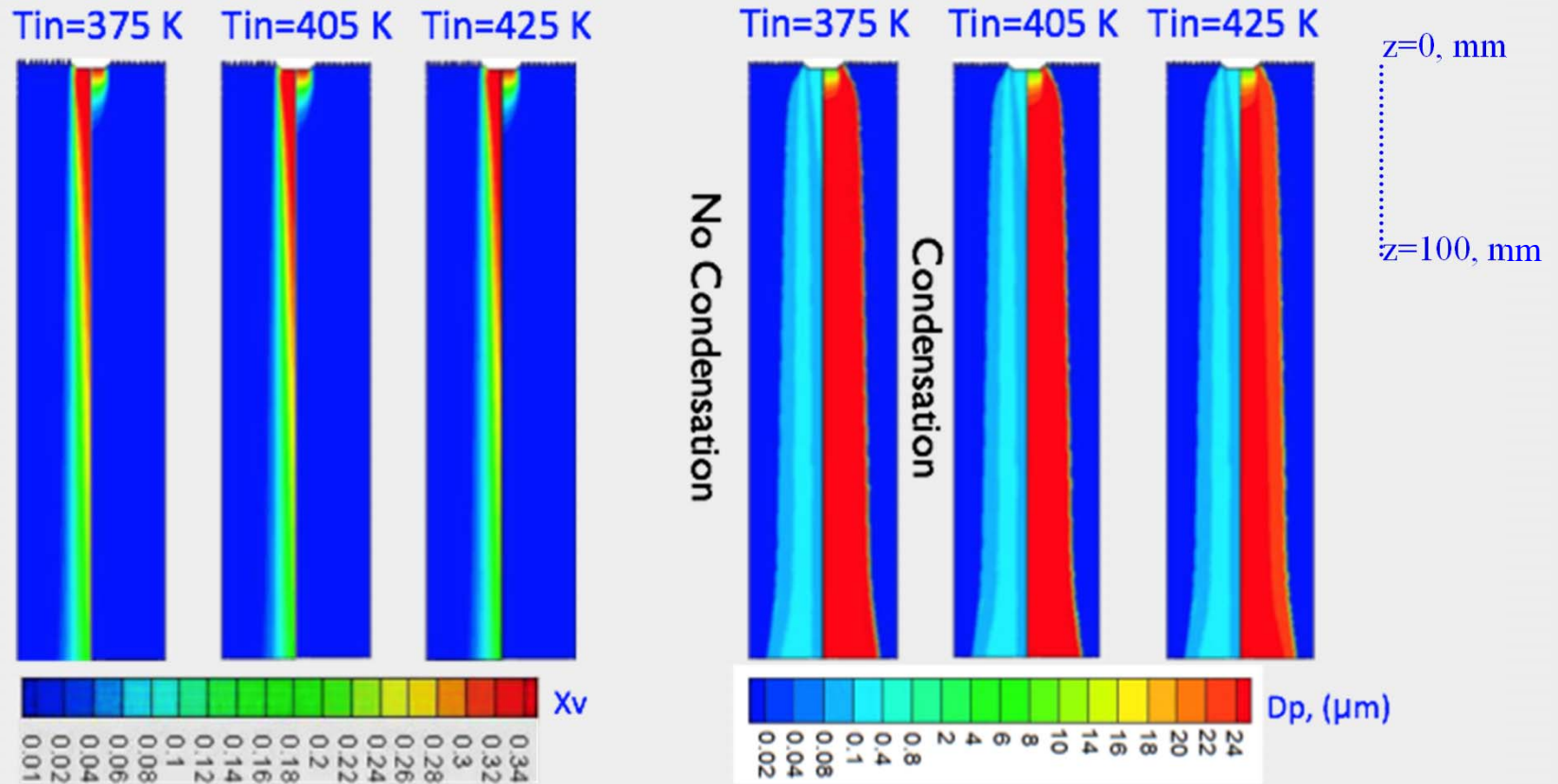


FPM (Fine particle model) is a set of User Defined Function solving aerosol continuity equation and allows the simulation of aerosol formation, growth and transport of particles

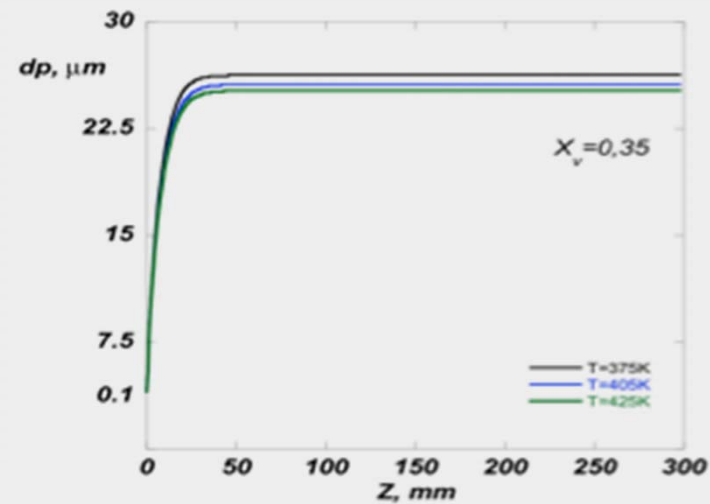
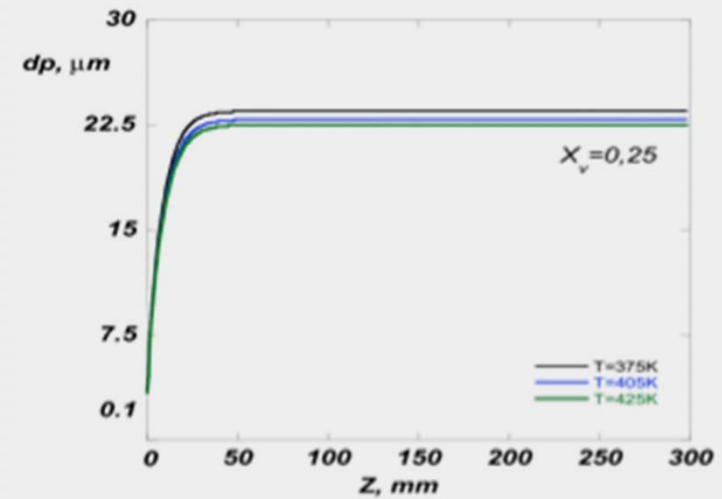
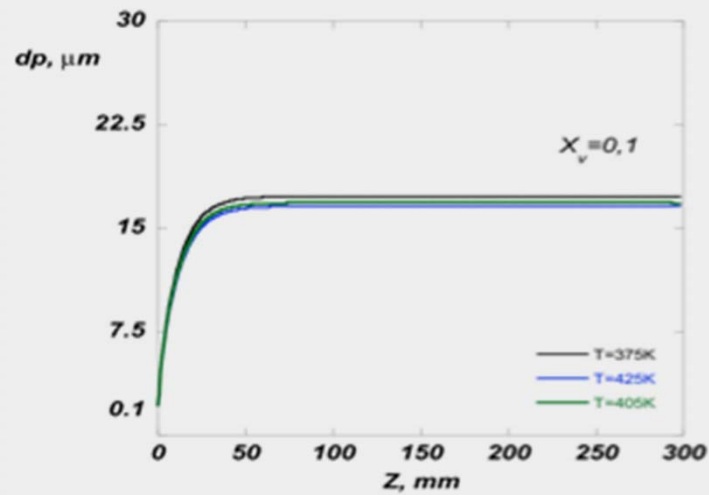
Numerical results $X_v=10\%$



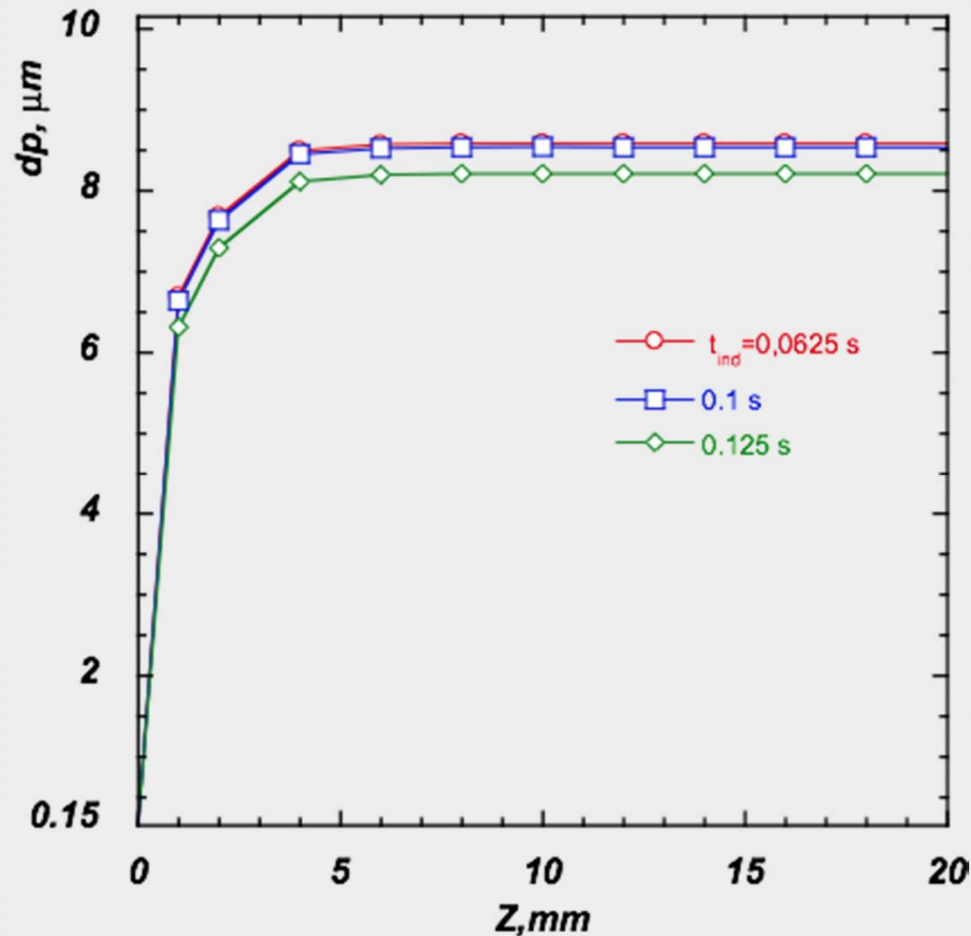
Numerical results $X_v=35\%$



Particle diameter -axial profiles

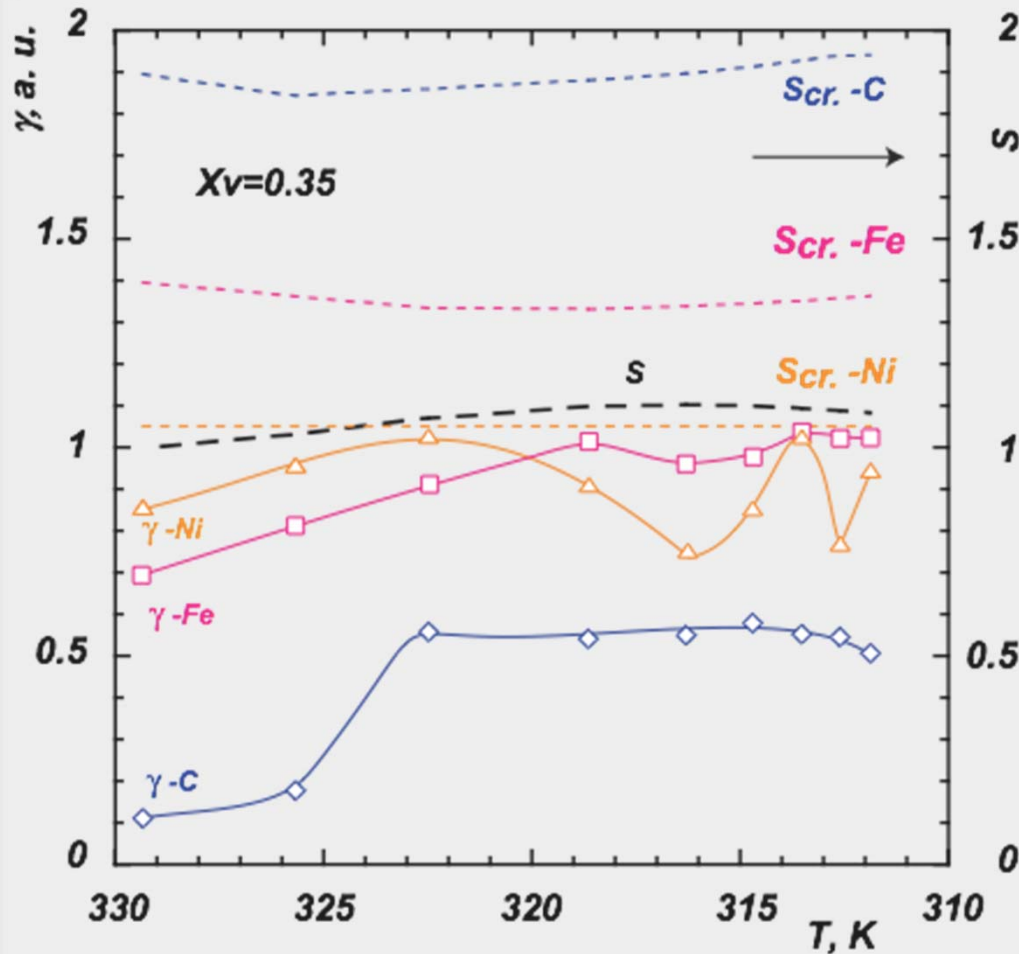


Simulation of condensational growth



✓ In all operating conditions considered the model (Barret and Clement, J. Aerosol Sci., 1988) is not able to predict induction time of the process

Nucleation activation



✓ Theoretical prediction of the nucleation activation can be used to determine the process effectiveness at higher X_v and lower T_{in} , even though it fails to predict the induction time.

✓ At low values of X_v , this approach was not valid in predicting the occurrence of particle size growth

Tools

The analysis of the evolution of the process of heterogeneous nucleation was carried out in experimental apparatus realized ad hoc which has requested:

- ✓ *Exploitation of nucleation theory*
- ✓ *Design of experimental configuration*
 - ▶ *Numerical modeling*
- ✓ *Set-up of experimental apparatus*
 - ▶ *diffusion cloud chamber*
 - ▶ *particulate generation system with high reproducibility and stability in terms of size and number concentration and flexible with respect to material type of particles produced*
 - ▶ *steam generation system*



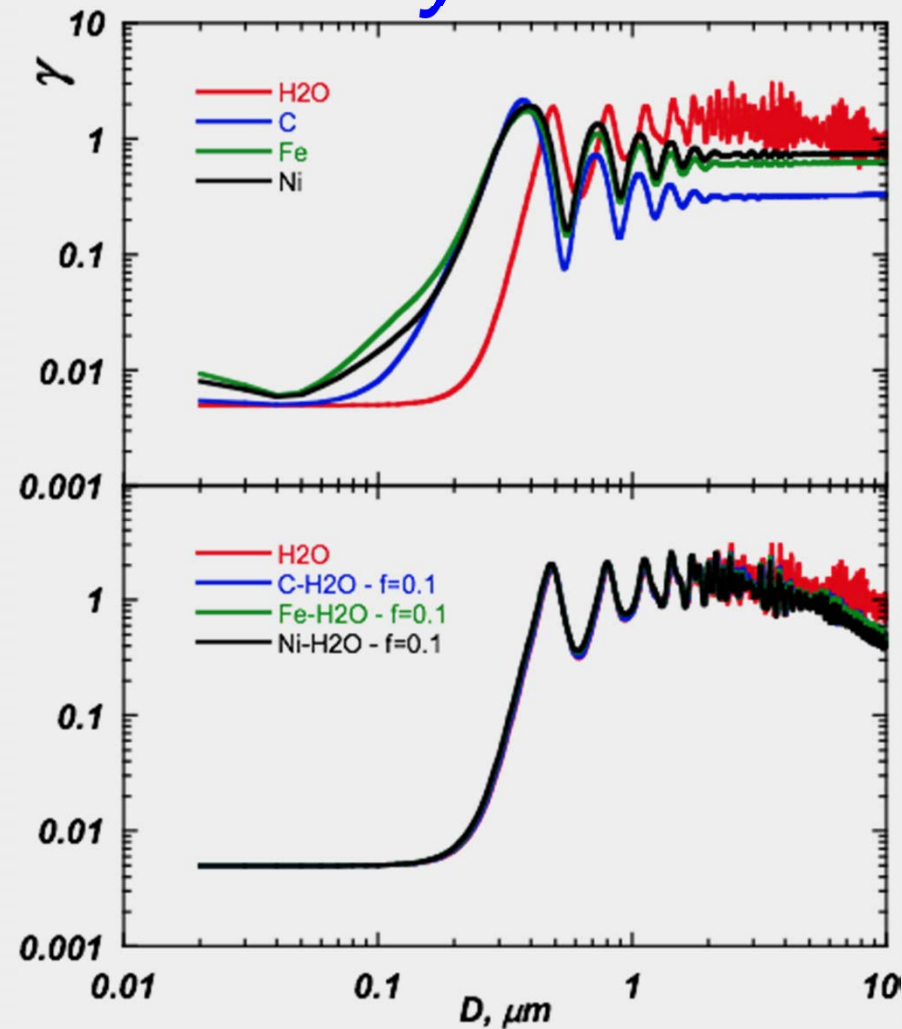
system for optical diagnostics

monitoring, control and automation

17th ETH Conference on Combustion Generated Nanoparticles- Zurich, June 23rd – 26th, 2013



Particle coverage - effect of water layer



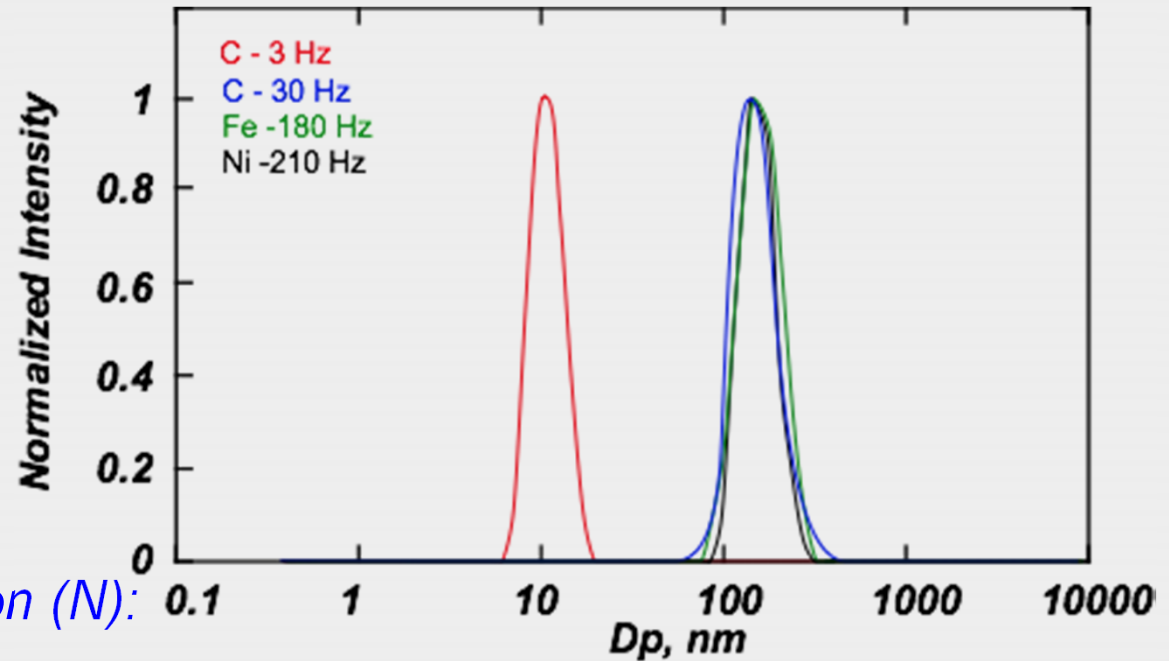
Gorden Videen, Petr Chylek, Optic Communication 1998



Particles characterization

✓ Particle Size (D_p):

➔ Malvern Zeta-sizer



✓ Number Particle Concentration (N):

➔ Low Pressure Electrostatic Impactor



Effect of vapor concentration

